Regular Article - Theoretical Physics

Half-wormholes and ensemble averages

Cheng Peng[a], **Jia Tian**[b], **Yingyu Yang**[c]

Kavli Institute for Theoretical Sciences (KITS), University of Chinese Academy of Sciences (UCAS), Beijing 100190, China

Abstract Recently, the concept of half-wormholes is introduced to give a resolution to the factorization puzzle in holography and help understand better the relation between ensemble average theories and gravity in the bulk. Half-wormholes are proposed to be the contributions to the gravitational path integral that correspond to fluctuations of each individual theory around the average of the whole ensemble of theories. In this paper, we further explore the extent to which the half-wormhole interpretation is applicable. In particular, to further demonstrate that the half-wormhole interpretation is not merely a feature of a specific theory but is a general feature of ensemble average theories, we examine various models, including different enriched 0-dimensional SYK-like models, the 1-dimensional Brownian SYK model and its generalization. To further demonstrate that the half-wormhole interpretation applies to more general probability distributions apart from the zero-mean Gaussian distribution, we consider random couplings with other non-trivial moments. Specifically, introducing a non-trivial mean value to the random coupling renders the spectral correlators to exhibit both disconnected saddles and connected saddles. The inclusion of higher-order moments leads to new "multi-linked half-wormhole" saddles. We also clarify the distinctions between the unlinked half-wormhole and the linked half-wormhole in our modified Brownian SYK model.

1 Introduction

The AdS/CFT correspondence [1–3] provides a non-perturbative definition of quantum gravity. An important lesson from the recently progress in understanding the black hole information paradox is that a summation of different configurations in the semi-classical gravitational path integral is crucial to probe some quantum mechanical properties of the system, such as the Page curve [4–7], the late-time behavior of the spectral form factor [8,9], and correlation functions [10,11], see also a recent review [12]. However, the inclusion of spacetime wormholes leads to an apparent factorization puzzle [13]; a holographic computation of the correlation functions of field theory partition functions living on different boundaries gives non-factorized results, i.e. $\langle Z_L Z_R \rangle \neq \langle Z_L \rangle \times \langle Z_R \rangle$, which is in tension with the general expectation on the field theory side. This revitalizes the hypothetical connection between wormholes and ensemble averages [14–17], and motivates an appealing conjectural duality between a bulk gravitational theory and (the average of) an ensemble of theories on the boundary [8,18–64], whose prototype is the by-now well known duality between the two-dimensional Jackiw-Teitelboim (JT) gravity [65,66] and the Schwarzian sector of the Sachdev-Ye-Kitaev (SYK) model [67–69], or more directly the random matrix theories [8,18]. These results suggest that solving the factorization problem could shed light on the microscopic structure of quantum gravity that are not universal and hence cannot be captured by the ensemble-averaged quantities [70,71]. In [72], the factorization problem is carefully studied in a toy model introduced in [52], where it is shown that the (approximate) factorization can be restored if other half-wormhole contributions are included. In the dual field theory analysis, these half-wormhole contributions are identified with non-self-averaging saddle points in each individual theory of the ensemble. This idea is explicitly realized in a 0-dimensional "one-time" SYK model in [73], followed by further analyses [74–81]. An explicit connection between the gravity computation in [72] and the field theory computation in [73] is proposed in [59].

In this paper, we explore the extent to which the half-wormhole interpretation is applicable.

[a] e-mail: pengcheng@ucas.ac.cn (corresponding author)

[b] e-mail: wukongjiaozi@ucas.ac.cn

[c] e-mail: yangyingyu18@mails.ucas.ac.cn

In Sect. 2, we first review the computation in [73] and provided another way to derive the same result. Our discussion is based on a detailed Lefschetz thimble analysis, which is independent of the argument given in [73]. The Lefschetz thimble analysis gives a systematic way to justify how to identify the correct set of saddle points to be included in the path integral. This serves as a very non-trivial cross-check of the result in [73] and a preparation for the later parts of this paper.

In Sect. 3, we consider a 0d SYK model whose random couplings are drawn from a probability distribution with a non-zero mean. The motivation to study this model is the following. The 0d SYK model studied in [73] is simple enough to explicitly demonstrate the contribution from half-wormholes, but some crucial properties of the more familiar 1d SYK model are missing in this 0d toy model. The most notable consequence of this is that the averaged partition function $\langle z \rangle$ of the 0d toy model in [73] is zero, so there is no disconnected contribution to any spectral correlation functions at all. This is quite different from the original 1d SYK model and hence raises a question if the conclusion obtained in the 0d model in [73] applies to the more familiar 1d SYK and other similar models. Our analysis in this section is a first step towards a thorough study of this question and a resolution of the factorization in that case. Our analysis shows that in the presence of a non-zero mean value of the random couplings, the structure of half-wormhole-like contributions is much richer, and in particular new types of non-self-averaging contributions become important and should be considered in the saddle point analysis of the spectral correlation functions.

In Sect. 4, we consider other generalized 0d SYK models whose random couplings are drawn from more general probability distributions other than the zero-mean Gaussian distribution. The motivation for this study is the following. First of all, a significant feature in the analysis of [73,77] is the Gaussian property of the randomness in the ensemble average model. On the other hand, the gravitational analysis [72] of a topological model [52] reveals that other connected half-wormhole configurations, which contain more than two half-wormholes linking together (see discussion around Figure 18 and in section 6.1 of [72]), play a crucial role in understanding the factorization problem in the gravity theory. This raises the question of whether there are similar multi-boundary linked-half-wormhole contributions in the boundary ensemble average theories. This motivates us to consider random couplings drawn from continuous distributions with non-trivial higher moments, which is a natural origin of non-trivial interconnections between the different factors of the spectral correlation functions. Furthermore, the results of the gravitational analysis in the toy model [52] suggest that a good boundary dual description could involve an ensemble average of different theories with Poisson distributions. A related anal-

ysis in [82] shows that random variables drawn from Poisson distributions have a natural connection to gravitational systems. Ensemble-averaged theories involving an average over uniform distributions on the moduli space [36–40,46,62,63] are shown to have clear connection to gravitational system. These motivate us to consider 0d SYK models with random couplings drawn from discrete distributions. Our computation shows that in theories with non-trivial higher moments, there are very rich structures of the non-self-averaging contributions to the spectral correlation functions, and the inclusion of higher moments yields new "multi-linked half-wormhole" saddles in addition to the original two-linked half-wormhole saddle. All these new saddle points should be taken into account in order to solve the factorization puzzle in these models. In addition, we find that when the random couplings are Poisson distributed, the multi-linked half-wormhole contributions are all suppressed in the large-N limit; contributions with disk and cylinder topology are good enough to solve the factorization puzzle.

In Sect. 5, we study the 1d Brownian SYK model and its generalizations. Since the SYK model is originally defined in 1d, the computation in this section clearly helps further explore the important question of whether the half-wormhole interpretation of the non-self-averaging contributions to various spectral correlators applies to models in 1-dimensional spacetime. By an explicit computation, we confirm that there is indeed a similar decomposition of the partition function into the averaged contribution and a punctured-disk-like non-self-averaging contribution. This agrees with our expectation obtained from the computation in the 0d model in Sect. 3. The results in this section also provide direct evidence of the wide applicability of the half-wormhole type interpretation of the non-self-average contributions in general ensemble average theories.

2 SYK at one time point: the cylinder model

In this section, we study the half-wormhole contributions in the toy 0d SYK model that can be considered as the usual 0+1d SYK model at a single instant of time. We first briefly review the previous results in [73] and also in [74,77]; in Sect. 2.3.2 we provide a detailed study of the various saddle points via a Lefschetz-thimble analysis, which is also a useful preparation for the analysis of the other models in this paper.

2.1 SYK model with one time point

As in [73], we are interested in the following Grassmann integral[1]

$$z = \int \mathrm{d}^N \psi \, \exp(\mathrm{i}^{q/2} J_{i_1 \ldots i_q} \psi_{i_1 \ldots i_q}), \tag{1}$$

---

[1] In this paper, repeated indices are summed if no further explanation.

where $\psi_{i_1 \ldots i_q} = \psi_{i_1} \psi_{i_2} \ldots \psi_{i_q}$ and ψ_i are Grassmann variables. The number z can be understood as the partition function of $0 + 0$ dimensional analogue of SYK model. The random couplings $J_{i_1 \ldots i_q}$ is drawn from a Gaussian distribution

$$\langle J_{i_1 \ldots i_q} \rangle = 0, \tag{2}$$

$$\langle J_{i_1 \ldots i_q} J_{j_1 \ldots j_q} \rangle = t^2 \delta_{i_1 j_1} \ldots \delta_{i_q j_q}, \quad t^2 = \frac{(q-1)!}{N^{q-1}}. \tag{3}$$

We sometimes use the collective indies A, B to represent a series of q indices to simplify our notation

$$A = \{i_1 < \cdots < i_q\}, \qquad J_A \psi_A \equiv J_{i_1 \ldots i_q} \psi_{i_1 \ldots i_q}. \tag{4}$$

Integrating out the Grassmann variables directly gives [2]:

$$z = \int \mathrm{d}^N \psi \exp(\mathrm{i}^{q/2} J_A \psi_A) \tag{5}$$

$$= \sum_{A_1 < \cdots < A_p}' \mathrm{sgn}(A) J_{A_1} \ldots J_{A_p}, \tag{6}$$

where $p = N/q$ and the expression (6) is the hyperPfaffian Pf(J) of the $J_{i_1 \ldots i_q}$ hypermatrix.

Before diving into the technical details, let us first outline the computation we will perform in this section. The ensemble theory (1) could be regarded as an effective description of a dual gravitational system. However, explicit computation uncovers a "factorization" problem of the spectral correlators (correlation functions of the partition functions), namely

$$\langle z^2 \rangle = \langle z_L z_R \rangle \neq f_L(z_L) f_R(z_R). \tag{7}$$

where we have trivially rewritten z^2 to $z_L z_R$ to emphasis that the two copies of z are independent to each other, and f_L, f_R are some functions. This leads to a puzzle: the correlation functions of the partition functions of two different theories are expected to factorize into two factors each only depends on one of the z's, but this is in contradiction with the above equation. In this section, we review a proposal [73] to resolve the puzzle and provide an independent computation by the Lefschetz-thimble method to support the results there. The main conclusion is that in the path integral of the spectral correlators, apart from the wormhole saddle that gives $\langle z_L z_R \rangle$, one should also include the contribution from another saddle point, which is referred to as the half-wormhole saddle, into the path integral. Then we have approximately

$$z^2 \approx \langle z_l z_R \rangle + \text{half-wormhole saddle}, \tag{8}$$

where the "half-wormhole saddle" is denoted by $\Phi(0)$ in the rest of this section.

---

[2] Here we choose the measure of Grassmann integral to be $\int \mathrm{d}^N \psi \, \psi_{1 \ldots N} = \mathrm{i}^{-N/2}$ and the prime on the sum means that in each term of the sum $A_i \cup A_j = \emptyset$ due to the fact $\psi^2 = 0$.

2.2 The ensemble averaged quantities

We first consider the ensemble averaged quantities $\langle z^2 \rangle$ which is defined as

$$z^2 = z_L z_R \tag{9}$$

$$= \int \mathrm{d}^N \psi^L \mathrm{d}^N \psi^R \exp \left\{ \mathrm{i}^{q/2} J_A \left(\psi_A^L + \psi_A^R \right) \right\}, \tag{10}$$

$$\langle z^2 \rangle = \int \mathrm{d}^{2N} \psi \exp \left\{ \frac{N}{q} \left(\frac{1}{N} \psi_i^L \psi_i^R \right)^q \right\}, \tag{11}$$

where we have assumed that q and N are even, and L, R labels the two copies of z on the left-hand-side. In the following, we would like to compute this quantity by saddle-point analysis. In the 0+1d SYK model, the analog of this quantity is the "spectral form factor" (SFF) $\langle Z(\beta + iT) Z(\beta - iT) \rangle$. It is known that both a "disk" saddle point and a "wormhole saddle" contribute to the SFF; the disk saddle is responsible for the decay of the SFF at the early time and the wormhole saddle is responsible for the linear increasing period called the "ramp" of the SFF in a relatively later time regime.

However, in the 0d SYK model there is no time. Moreover, since $\langle z \rangle = 0$, only a wormhole saddle is possible to exist. In the following, we will confirm the existence of the wormhole saddle by comparing the exact evaluation of $\langle z^2 \rangle$ and its saddle point approximation. The exact values of (11) can be computed by introducing a G variable

$$\langle z^2 \rangle = \int \mathrm{d}^{2N} \psi \int_{\mathbb{R}} \mathrm{d}G$$

$$\times \delta \left(G - \frac{1}{N} \sum_{i=1}^N \psi_i^L \psi_i^R \right) \exp \left(\frac{N}{q} G^q \right) \tag{12}$$

$$= N^{-N} \int_{\mathbb{R}} \mathrm{d}G \exp \left(\frac{N}{q} G^q \right) (-\partial_G)^N \delta(G) \tag{13}$$

$$= \frac{N! (N/q)^{N/q}}{N^N (N/q)!} \tag{14}$$

$$= e^{-(1-\frac{1}{q})N} \sqrt{q} \left(1 + \frac{1-q}{12N} + \mathcal{O}\left(\frac{1}{N^2} \right) \right), \tag{15}$$

where in the last step we expand to the next-to-leading order of $1/N$.

Next we derive the same result (15) from a saddle point approximation. We start by rewriting the δ function in (12)

$$\delta \left(G - \frac{1}{N} \sum_i \psi_i^L \psi_i^R \right) = \int \mathrm{d}\Sigma \, e^{\mathrm{i}\Sigma \left(G - \frac{1}{N} \psi_i^L \psi_i^R \right)}, \tag{16}$$

and then deform the contour of the integration along which the g, σ variables, defined by

$$\Sigma = \mathrm{i} e^{-\mathrm{i}\frac{\pi}{q}} \sigma, \quad G = e^{\mathrm{i}\frac{\pi}{q}} g, \tag{17}$$

are real. This modification ensures the convergence of the integral. The resulting effective action is

$$
\langle z^2 \rangle = \int_R \mathrm{d}g \int_R \frac{\mathrm{d}\sigma}{2\pi/N}
$$
$$
\times \exp \left\{ N \left(\log \left(\mathrm{i}e^{-\frac{\mathrm{i}\pi}{q}} \sigma \right) - \mathrm{i}\sigma g - \frac{1}{q} g^q \right) \right\}, \quad (18)
$$

$$
\equiv \int_R \mathrm{d}g \int_R \frac{\mathrm{d}\sigma}{2\pi/N} e^{NS}. \quad (19)
$$

The saddle point equations of this path integral are

$$
-\mathrm{i}\sigma - g^{q-1} = 0, \quad g^q = -1, \quad (20)
$$

$$
\rightarrow \quad g = e^{\frac{(2m+1)\mathrm{i}\pi}{q}}, \quad m = 0, \ldots, q-1. \quad (21)
$$

All of them give the same on-shell action

$$
\langle z^2 \rangle_s = \frac{N}{2\pi} e^{-\left(1-\frac{1}{q}\right)N}. \quad (22)
$$

To match with the exact result (15) we need to add in contributions from fluctuations around each of these saddle points. For simplicity let us take $q = 4$ and focus on one of the saddle points

$$
\sigma_s = g_s = -(-1)^{\frac{3}{4}}, \quad \langle z^2 \rangle_s = \frac{N}{2\pi} e^{-\frac{3}{4}N}. \quad (23)
$$

Expanding the exponent around this saddle

$$
\sigma = \sigma_s + x, \quad g = g_s + y, \quad (24)
$$

to the 4th order

$$
S_2 \sim -\frac{3}{4} + \frac{3\mathrm{i}x^2}{2} - \mathrm{i}xy - \frac{\mathrm{i}y^2}{2}
$$
$$
+ \left[(-1)^{3/4} x^3 + \frac{(-1)^{3/4}}{3} y^3 \right] \epsilon + \frac{y^4 - x^4}{4} \epsilon^2, \quad (25)
$$

where we have added $\epsilon \equiv 1$ to keep track of the expansion, then expanding $\exp(S_2)$ to the second order of ϵ and finally evaluating the integral (18) to this order directly gives the contribution from this saddle up to 2-loop as

$$
\langle z^2 \rangle_{\text{saddle+loop}} = e^{-\frac{3}{4}N} \frac{1}{2} \left(1 - \frac{1}{4N} \right). \quad (26)
$$

Adding contributions from all the 4 saddles we arrive at

$$
\langle z^2 \rangle_{\text{saddle+loop}} = 2e^{-\frac{3}{4}N} \left(1 - \frac{1}{4N} \right), \quad (27)
$$

that agrees with (15) at 2-loop order. These saddles are named as the wormhole saddles because in the 0+1d SYK model, they have a gravity dual which can be viewed as a wormhole.[3]

At first glance, it may be surprising that we need to add all complex saddle points (which are not along the integral contour along the real axis) to obtain the correct result. However

---

[3] More precisely, the gravity dual is the double-cone geometry.

this can be explained and justified with the method of Lefschetz thimbles which we discuss in Sect. 2.3.2 with some technical details reviewed in Appendix A. The method of Lefschetz thimbles is a way to determine which saddle points should be considered when there are multiple saddle points in the integral domain. In short, for each saddle point we can associate a steepest descent path which is called the Lefschetz thimbles and if the thimble intersects with the chosen integral contour then the corresponding saddle point should be included.

2.3 The non-averaged quantities

Now we try to compute the non-averaged quantity (10) in the saddle point approximation. Following [73], we rewrite z^2 as an integral

$$
z^2 = \int_R \mathrm{d}\sigma \, \Psi(\sigma) \Phi(\sigma), \quad (28)
$$

$$
\Psi(\sigma) = \int \frac{\mathrm{d}g}{2\pi/N} \exp[N(-\mathrm{i}\sigma g - 1/qg^q)], \quad (29)
$$

where the coupling dependent piece Φ is

$$
\Phi(\sigma) = \int \mathrm{d}^{2N} \psi \exp \left\{ \mathrm{i}e^{-\frac{\mathrm{i}\pi}{q}} \sigma \psi_i^L \psi_i^R + \mathrm{i}^{q/2} J_A \left(\psi_A^L + \psi_A^R \right) \right.
$$
$$
\left. - \frac{N}{q} \left(\frac{1}{N} \psi_i^L \psi_i^R \right)^q \right\}. \quad (30)
$$

This expression (28) is derived by inserting the trivial identity $1 = \int \mathrm{d}G \delta(G - 1/N \sum_i \psi_i^L \psi_i^R)$ and rotating the contour. In this form, the ensemble average of $\langle z^2 \rangle$ is entirely attributed to the ensemble average of $\Phi(\sigma)$

$$
\langle z^2 \rangle = \int_R \mathrm{d}\sigma \, \Psi(\sigma) \langle \Phi(\sigma) \rangle, \quad (31)
$$

since the $\Psi(\sigma)$ does not depend on the random couplings.

The integral region of (28) can be divided into two subregions depending on whether $\Phi(\sigma)$ is self-averaging or not. By self-averaging we mean the fluctuations around the average value is small in the large N limit

$$
\Phi(\sigma) - \langle \Phi(\sigma) \rangle \approx 0, \quad \Leftrightarrow \quad \langle (\Phi(\sigma) - \langle \Phi(\sigma) \rangle)^2 \rangle \approx 0,
$$
$$
\Leftrightarrow \quad \langle \Phi(\sigma)^2 \rangle \approx \langle \Phi(\sigma) \rangle^2. \quad (32)
$$

If the wormhole saddle points (20) are in this subregion, we then know that the result of the integral (28) is self-averaging, namely it can be approximated as $\langle z^2 \rangle \approx \langle z^2 \rangle_{\text{wormhole-saddle}}$. In this simple model, both $\langle \Phi(\sigma) \rangle$ and $\langle \Phi(\sigma)^2 \rangle$ can be computed exactly. The $\langle \Phi(\sigma) \rangle$ can be directly obtained as

$$
\langle \Phi(\sigma) \rangle = (\mathrm{i}e^{-\frac{\mathrm{i}\pi}{q}} \sigma)^N. \quad (33)
$$

To compute $\langle \Phi(\sigma)^2 \rangle$, we introduce σ_{AB} and g_{AB} analogous to (17)

$$g_{AB} = e^{-i\frac{\pi}{q}} G_{AB}, \quad G_{AB} = \frac{1}{N} \sum_i \psi_i^A \psi_i^B, \qquad (34)$$

where we label the L, R in one of the $\Phi(\sigma)$ (30) by $L = 1, R = 2$, and L', R' in the other of the $\Phi(\sigma)$ by $L' = 3, R' = 4$. Then the combination (AB) is one of $\{(13), (14), (23), (24)\}$. Each g_{AB} is paired with a σ_{AB} whose subscript has the same meaning as in g_{AB}. Then similar to the computation we used to get (15), $\langle \Phi(\sigma)^2 \rangle$ can be done exactly

$$\langle \Phi(\sigma)^2 \rangle$$
$$= \int_R \frac{d^4\sigma_{AB} d^4 g_{AB}}{(2\pi/N)^4} \exp\left\{ N \left[\log(-e^{-\frac{2i\pi}{q}}(\sigma^2 \right.\right.$$
$$\left.\left. +\sigma_{14}\sigma_{23} - \sigma_{13}\sigma_{24})) - i\sigma_{AB}g_{AB} - \frac{1}{q} g_{AB}^q \right] \right\}, \qquad (35)$$

$$= (-e^{-\frac{2i\pi}{q}})^N \sum_{n_1+n_2+n_3=\frac{N}{q}, n_i \geq 0} \frac{N!}{N^{2q(n_2+n_3)}}$$
$$\times \left(\frac{N}{q}\right)^{2(n_2+n_3)} \frac{\sigma^{2qn_1}(qn_2)!(qn_3)!}{(qn_1)!(n_2!)^2(n_3!)^2}, \qquad (36)$$

It can be organized into a polynomial in σ

$$\langle \Phi(\sigma)^2 \rangle = (-e^{-\frac{2i\pi}{q}})^N \left(\sigma^{2N} + \frac{2N!q!}{(N-q)!q^2 N^{2q-2}} \sigma^{2N-2q} \right.$$
$$\left. + \cdots + e^{2N\frac{1-q}{q}} 2q \right) \qquad (37)$$

$$\sim (-e^{-\frac{2i\pi}{q}})^N \left(\sigma^{2N} + \frac{2(q-1)!}{q N^{q-2}} \sigma^{2N-2q} \right.$$
$$\left. + \cdots + e^{2N\frac{1-q}{q}} 2q \right), \qquad (38)$$

where the phase factor is trivial whenever q divides N. Apparently when $q > 2$ and $\sigma^{2q} N^{q-2} \gg 1$ we have

$$\langle \Phi(\sigma)^2 \rangle \approx \langle \Phi(\sigma) \rangle^2, \qquad (39)$$

and the result is self-averaging.

In this simple example, we can perform an exact computation to get the results. However, in other models there is not a similar exact computation so it is important to understand how to reach the same conclusion by saddle approximation.

2.3.1 The saddle points analysis: $\sigma \neq 0$, the trivial saddle

The saddle point equations of the integral (35) are

$$g_{AB}^{q-1} = -i\sigma_{AB}, \quad -ig_{13} = \frac{\sigma_{24}}{f}, \quad ig_{14} = \frac{\sigma_{23}}{f},$$
$$ig_{23} = \frac{\sigma_{14}}{f}, \quad -ig_{24} = \frac{\sigma_{13}}{f}, \qquad (40)$$

where $f \equiv \sigma_{14}\sigma_{23} - \sigma_{13}\sigma_{24} + \sigma^2$. The above set of equations has a trivial solution $\sigma_{AB} = g_{AB} = 0$, which we call the "trivial saddle". The trivial saddle point value of $\langle \Phi(\sigma)^2 \rangle$ is

$$\langle \Phi(\sigma)^2 \rangle_{\text{trivial}} = \left(\frac{N}{2\pi}\right)^4 \left(-e^{-\frac{2i\pi}{q}}\sigma^2\right)^N = N^4 \langle \Phi(\sigma) \rangle^2, \qquad (41)$$

and the 1-loop fluctuations around the trivial saddle points is $1/N^4$ suppressed. Therefore the contribution up to 1-loop level is

$$\langle \Phi(\sigma)^2 \rangle_{\text{trivial+1loop}} = (-e^{-\frac{2i\pi}{q}}\sigma^2)^N = \langle \Phi(\sigma) \rangle^2, \qquad (42)$$

which says the trivial saddle always agrees with the first term in (37). If this saddle dominates the integral the quantity z^2 is self-averaging.

2.3.2 The saddle points analysis: $\sigma \neq 0$, the wormhole saddle

However, there could be other non-trivial solutions to the saddle point equation (40) with $\sigma_{AB} \neq 0$. From the equations of motion we obtain

$$x^{q-2} = y^{q-2}, \qquad (43)$$
$$(x^{q-1} - y^{q-1} + \sigma^2)^2 = x^{q-2} = y^{q-2}, \qquad (44)$$
$$g_{13}^q = g_{24}^q, \quad g_{23}^q = g_{14}^q \qquad (45)$$

where

$$x = g_{13}g_{24}, \quad y = g_{14}g_{23}. \qquad (46)$$

It is easy to check that solutions of the above equation satisfy $x = ye^{\frac{2m\pi i}{q-2}}$, and for each choice of m there are $2q^2$ solutions of g_{ab}.

For simplicity, we again focus on the $q = 4$ case, where there are only two classes of solutions $x = \pm y$.

• When $x = y$ we find 32 non-trivial saddles. The on-shell action of them are all the same

$$\langle \Phi(\sigma)^2 \rangle_{\text{non-trivial}}^+ = N^4 \langle \Phi(\sigma) \rangle^2 = \langle \Phi(\sigma)^2 \rangle_{\text{trivial}}, \qquad (47)$$

where the factor N^4 comes from the measure of (35). However, the one-loop fluctuations around these non-trivial saddle points amount to one-eighth of the fluctuations from the trivial saddle, with a value of $1/(8N^4)$. Although when the 1-loop effects are taken into account, we observe that the trivial saddles give larger contributions. But the contributions from the non-trivial saddles are also significant. Therefore naively we should add the contributions from all these saddle point, however, if we were adding the contributions from both the trivial and non-trivial saddles the answer would exceed the exact value (37). This suggests that only a subset of these
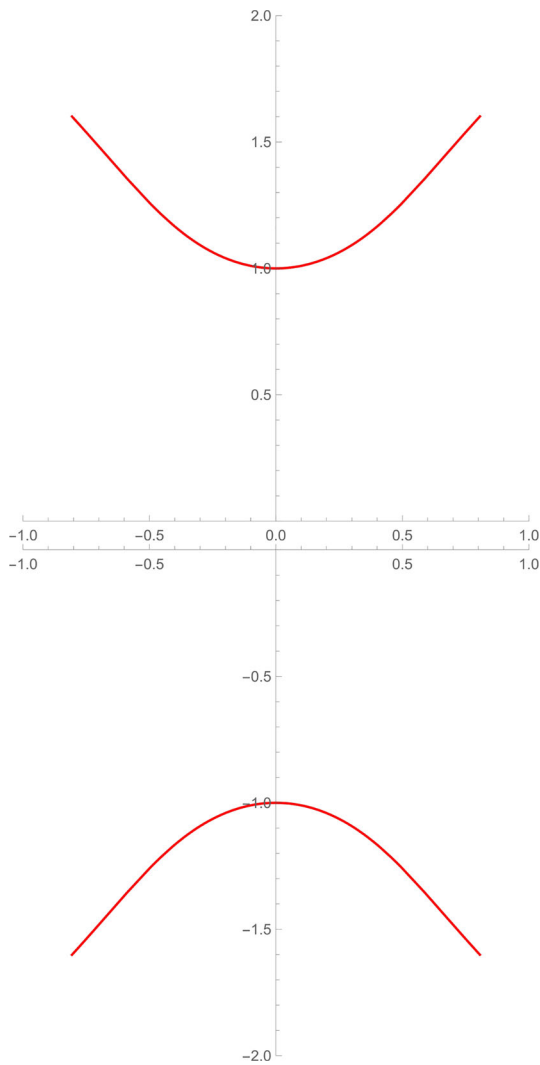
Fig. 1 Anti-thimble on the σ_{13} plane (left) and the σ_{24} plane (right)

saddle point contributions should be included in the integral expression of $\langle\Phi(\sigma)^2\rangle$. Indeed, through a straightforward Lefschetz-thimble analysis, as reviewed in Appendix A (see also [83]), we conclude that only trivial saddles are needed. The detailed reasoning is as follows.

To start with, we choose the real part of the action (35) as a Morse function

$$
\begin{aligned}
h &\equiv \Re(S) \\
&= \sum_{abj}\left(-\frac{g_{abj}^4}{4} + \frac{3g_{ab1}^2 g_{ab2}^2}{2} + g_{ab1}\sigma_{ab2} + g_{ab2}\sigma_{ab1}\right) \\
&\quad + \frac{1}{2}\log\left((\sigma_{142}\sigma_{231} + \sigma_{141}\sigma_{232} - \sigma_{132}\sigma_{241} - \sigma_{131}\sigma_{242})^2\right. \\
&\quad \left. +(1 + \sigma_{141}\sigma_{231} - \sigma_{142}\sigma_{232} - \sigma_{131}\sigma_{241} + \sigma_{132}\sigma_{242})^2\right),
\end{aligned}
\tag{48}
$$

where we have set $q = 4$ for simplicity and rescaled σ to 1 since we are interested in the case $\sigma \neq 0$. The g_{abi} and σ_{abj} are the real and imaginary parts of the field g_{ab} and σ_{ab}

$$
g_{ab} = g_{ab1} + ig_{ab2}, \quad \sigma_{ab} = \sigma_{ab1} + i\sigma_{ab2} . \tag{49}
$$

The downward flow equations of the Morse function are

$$
\frac{dg_{abj}}{dt} = -\frac{\partial h}{\partial g_{abj}}, \quad \frac{d\sigma_{abj}}{dt} = -\frac{\partial h}{\partial \sigma_{abj}} . \tag{50}
$$

The end point of each anti-thimble is one of the saddles, labeled by c, at g_{abj}^c and σ_{abj}^c, which leads to the following boundary conditions of the flow equation

$$
\lim_{t\to+\infty} g_{abj} = g_{abj}^c, \quad \lim_{t\to+\infty}\sigma_{abj} = \sigma_{abj}^c . \tag{51}
$$

We can then solve the flow equation and obtain the Lefschetz anti-thimbles going through each saddle point. If they intersect with the original integration contour the saddle point contributes to the integral.

For example in Fig. 1 we illustrate examples of the anti-thimbles of the saddle point

$$
g_{13} = 1, \quad g_{24} = -1, \quad g_{14} = (-1)^{3/4}, \quad g_{23} = (-1)^{1/4}, \tag{52}
$$

$$
\sigma_{13} = i, \quad \sigma_{24} = -i, \quad \sigma_{14} = (-1)^{3/4}, \quad \sigma_{23} = -(-1)^{1/4}, \tag{53}
$$

which do not intersect with the original integration contour, namely the real axis. This means the contribution of this saddle should not be included in the integral.

Examples of anti-thimbles of another saddle point

$$
g_{13} = -(-1)^{1/4}, \quad g_{24} = (-1)^{3/4}, \quad g_{14} = -1, \quad g_{23} = -1, \tag{54}
$$

$$
\sigma_{13} = (-1)^{1/4}, \quad \sigma_{23} = (-1)^{3/4}, \quad \sigma_{14} = -i, \quad \sigma_{23} = -i, \tag{55}
$$

is shown in Fig. 2. Again they do not intersect with the real axis so the contribution from this saddle should not be included either.

We can run this analysis over all the nontrivial saddles, and we find none of them contribute to the integral.

• When $x = -y$, there are also nontrivial saddle points, and a similar analysis of Lefschetz-thimbles demonstrates that they do not contribute to the integral either.

Actually, there is a quicker way to arrive at the same conclusion. We find that the on-shell actions corresponding to these saddle points are

$$
\left(\frac{\sigma^2}{2}\right)^{\frac{N}{3}} e^{-N \pm \frac{3}{2} 2^{\frac{1}{3}} N e^{\frac{2im\pi}{3}}\sigma^{\frac{4}{3}}}, \quad m = 0, \pm 1. \tag{56}
$$

Fig. 2 Anti-thimble on the g_{13} plane (left) and the g_{24} plane (right)

However, these saddle points should be saddle points of the entire multi-dimensional integral including the integral over σ. As a result, this saddle should also satisfy the fall-off condition of the σ integral, otherwise, they will not contribute to the σ integral. Therefore we should only consider the decaying saddle points namely

$$
\left(\frac{\sigma^2}{2}\right)^{\frac{N}{3}} e^{-N+\frac{3}{2}2^{\frac{1}{3}}Ne^{\pm\frac{2i\pi}{3}}\sigma^{\frac{4}{3}}}, \quad \left(\frac{\sigma^2}{2}\right)^{\frac{N}{3}} e^{-N-\frac{3}{2}2^{\frac{1}{3}}N\sigma^{\frac{4}{3}}}.
$$
(57)

We plot the region where these non-trivial saddle dominates over the trivial saddle in Fig. 3, and it is easy to observe from the figure that the wormhole saddle (20) of $\langle z^2 \rangle$, located at $|\sigma| = 1$, is in the region where the trivial saddle dominates.
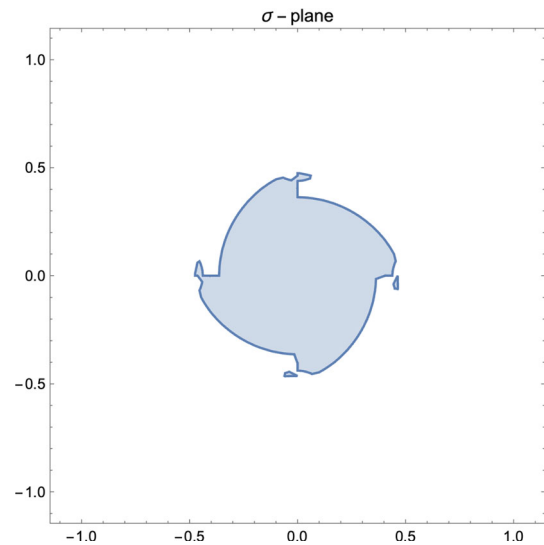
Fig. 3 The shaded region is where a non-trivial saddle in (56) dominates over the trivial saddle. The plot for the other two non-trivial saddles can be obtained from this plot by simple rotations

Another family of solutions to the equation of motion (40) has $x = 0$ or $y = 0$. On shell actions on these saddles behave as

$$
\sigma^{\frac{2N}{3}} e^{-N+\frac{3}{2}Ne^{\pm\frac{2i\pi}{3}}\sigma^{\frac{4}{3}}}, \quad \sigma^{\frac{2N}{3}} e^{-N-\frac{3}{2}N\sigma^{\frac{4}{3}}},
$$
(58)

whose dominant regions are similar to Fig. 3 and they are sub-leading compared with the trivial saddle.

Since the trivial saddle is on the original integration contour, putting all the results together we confirm that the path integral over g_{ab} and σ_{ab} can be approximated entirely by the trivial saddle point. Due to (42), we conclude that the wormhole saddle (20) is in the self-averaging region.

2.3.3 The saddle points analysis: $\sigma = 0$, the half-wormhole saddles

The analysis in the above sub-sections concludes that the leading saddle point contributions to the $\Phi(\sigma)$ function are all proportional to positive powers of σ. However, this raises a puzzle: all these results vanish at $\sigma = 0$, but from the exact result in (37) we know

$$
\langle \Phi(0)^2 \rangle_{\text{exact}} \sim 2q e^{-\frac{3}{2}N} \neq 0.
$$
(59)

at $\sigma = 0$. This indicates that there must be other saddle points, which are missed in the previous analysis due to being subleading at generic $\sigma \neq 0$, becomes important at $\sigma = 0$. This is possible because in the large-N limit the $\Psi(\sigma)$ function is peaked at the origin, so other saddle points could give a large contribution near the origin. In this section, we thus focus on the $\sigma \sim 0$ region of the integration and look for new saddle point contributions.

In practice, we can apply the same analysis as in the previous section, except that now we evaluate at $\sigma \sim 0$. As expected, the trivial saddle gives

$$e^{N \log(\sigma)} \sim 0 \, . \tag{60}$$

At $\sigma = 0$, the subleading non-trivial saddles (57) and (58) discussed in the previous section now have different on-shell values

$$\frac{e^{-\frac{3}{2}N}}{2^{N/2}}, \quad e^{-\frac{3}{2}N} \, , \tag{61}$$

respectively. So (58) dominates. Adding them up and including the 1-loop correction, the result agrees precisely with the exact solution (59)

$$\langle \Phi(0)^2 \rangle = 2q e^{-\frac{3}{2}N} \, . \tag{62}$$

We can continue to carry out the sigma integral to get the contribution from this saddle to the z^2, since the saddle is supported at $\sigma = 0$, this is easily done the result is simply $\Phi(0)$.

A general lesson we can learn from this computation is that the half-wormhole saddle points always exist. But most of the time they are hidden behind the leading saddles. Nevertheless, they become important whenever the leading saddle decreases faster, e.g. the $\sigma \sim 0$ region in this case.

With both the wormhole and the half-wormhole saddle contributions, we can now approximate

$$z^2 \approx \langle z^2 \rangle + \Phi(0) \, . \tag{63}$$

The wormhole saddle is holographically dual to bulk wormhole-like geometry, and the half-wormhole saddles are conjectured to be dual to half-wormhole-like configurations that are typically sub-dominant. This result indicates one way to resolve the factorization problem; when we consider bulk gravitational path integral, the factorization problem is caused by only considering the wormhole-like connected geometry, if other sub-dominant contributions, such as the half-wormhole geometries are also taken into account, the factorization property will be restored (so that the result is $z^2 \equiv z_L z_R$ that factorizes).

3 Sourced one-time SYK: a disk-and-cylinder model

An important difference between the 0d-SYK model and the 1d-SYK model is that the averaged partition function $\langle z \rangle$ vanishes in the 0d model. From the bulk gravity point of view, this corresponds to the exclusion of the gravity configuration where a surface with the disk topology fills a single boundary

in the bulk. as shown in [72]. JT gravity admits a limit where the bulk geometry can always be approximated by disks and cylinders. Therefore to understand if the discussion in the previous model is also applicable when disk topology is also allowed in the bulk, we consider a sourced 0d-SYK model where the random coupling is drawn from a Gaussian distribution $\mathcal{N}(u, t^2)$ with non-zero mean[4]

$$\langle J_A \rangle = J_A^0 = u, \quad \langle J_A^2 \rangle - \langle J_A \rangle^2 = \tau^2 \frac{(q-1)!}{N^{q-1}} \equiv t^2. \tag{64}$$

Since a non-zero expectation value of the couplings is equivalent to turning on a source term of the random couplings, we call this model "sourced" 0d-SYK model.

The ensemble averaged quantities can be computed directly by averaging over the couplings and integrating out the fermions

$$\langle z \rangle = \mathrm{PF}(J^0), \tag{65}$$

$$\langle z^2 \rangle = \int \mathrm{d}^{2N} \psi$$

$$\times \exp\left(i^q t^2 \sum_A \psi_A^L \psi_A^R + i^{q/2} J_A^0 \left(\psi_A^L + \psi_A^R \right) \right) \tag{66}$$

$$= \sum_{A,B}' \mathrm{sgn}(A)\mathrm{sgn}(B) \left(J_{A_1}^0 J_{B_1}^0 + \delta_{A_1 B_1} t^2 \right) \cdots$$

$$\cdots \left(J_{A_p}^0 J_{B_p}^0 + \delta_{A_p B_p} t^2 \right). \tag{67}$$

Our main results about this model are

1. The self-averaging part of z does not persist; they are subdominant compared with the non-self-averaging contribution in the large N limit.
2. The half-wormhole contribution Φ can be improved so that the approximation $z^2 \approx \langle z^2 \rangle + \Phi$ is still good in this model.

3.1 The averaged quantities

Let us first compute the averaged quantities. We again proceed by looking for proper collective variables and establish a saddle point analysis that's similar to the model discussed in the previous section.

The ensemble average of z is simply the ensemble average of the hyperPfaffian (6)

$$\langle z \rangle = \sum_{A_1 < \cdots < A_p}' \mathrm{sgn}(A) J_{A_1}^0 \ldots J_{A_p}^0 = m[p]u^p, \tag{68}$$

where p is not summed over, $pq = N$ and the factor $m[p]$ is defined as

$$m[p] = \frac{(pq/2)!}{p!((q/2)!)^p}. \tag{69}$$

This result can alternatively be derived by introducing a collective variable

$$G = \sum_{i<j} \psi_i \psi_j, \tag{70}$$

followed by a similar computation as we show in (15). Introducing the following collective variables

$$G_{LR} = \frac{1}{N} \sum_i \psi_i^L \psi_i^R, \tag{71}$$

$$G_L = \frac{1}{N} \sum_{i<j} \psi_i^L \psi_j^L, \quad G_R = \frac{1}{N} \sum_{i<j} \psi_i^R \psi_j^R, \tag{72}$$

we can compute the averaged quantity $\langle z^2 \rangle$

$$\langle z^2 \rangle = \sum_{k=0}^{p} c[k] t^{2k} \left(m[p-k] u^{p-k} \right)^2, \tag{73}$$

where $m[p]$ is defined in (68) and the coefficient $c[k]$ is

$$c[k] = \frac{1}{k!} \binom{N}{q} \binom{N-q}{q} \cdots \binom{N-(k-1)q}{q} \tag{74}$$

$$= \frac{N!}{k!(q!)^k (N-kq)!}. \tag{75}$$

The details of the derivations of $\langle z \rangle$ and $\langle z^2 \rangle$ are presented in Appendix B. The averaged partition function (68) is proportional to u^p because in each term of the hyperPfaffian there are no repeated J_{A_i} so the result does not depend on t; rather, each random coupling has to "contract" with itself thus producing p copies of the factor of u. The polynomial expression of the averaged squared partition function (73) can be also understood from summing over the Feynman diagrams as shown in Fig. 5. It turns out that each diagram in Fig. 5 correpond to a term $z_2^{(k)}$ in (73), i.e.

$$\langle z^2 \rangle = \sum_{k=0}^{p} z_2^{(k)}, \quad z_2^{(k)} = c[k] t^{2k} \left(m[p-k] u^{p-k} \right)^2. \tag{76}$$

Diagramatically, the $z_2^{(k)}$ come as follows. We first contract k pairs of J_{A_i} (in the diagram the contraction is denoted by a blue line connecting z_L and z_R) which gives the factor t^{2k} and $c[k]$ is the total number of different contractions. Each of the rest J_A becomes μ in the average and they contribute a factor $\left(m[p-k] u^{p-k} \right)^2$ (in the diagram the contraction is denoted by a red line connecting z_L or z_R with a red dot.).

In the large-N limit, we can find the dominant terms by computing the ratio[5]

$$\begin{aligned} r_k &= \frac{z_2^{(k)}}{z_2^{(k-1)}} \\ &= \frac{t^2(-k+p+1)(-4k+4p+1)(-4k+4p+3)}{3u^2(2k(p-k)+k)} \end{aligned} \tag{77}$$

$$r_p = \frac{t^2}{pu^2}, \quad r_1 \sim \frac{p^2 t^2}{u^2}, \tag{78}$$

here for simplicity we have chosen $q = 4$. First we notice that r_k decreases with respect to k, namely

$$r_k > r_{k+1} \tag{79}$$

Therefore if $r_1 \ll 1$ i.e.

$$\frac{u}{t} \gg p, \tag{80}$$

then the dominant term will be

$$\langle z^2 \rangle \approx z_2^{(0)} = \left(m[p] u^p \right)^2. \tag{81}$$

In this case, we clearly have

$$\langle z^2 \rangle \approx \langle z \rangle^2. \tag{82}$$

Since the geometric meaning of $z_2^{(0)}$ is two disconnected disks, the above result means in this regime, this "two-disk" saddle is dominant, which results in a self-averaging z due to (82). This behavior resembles the early-time characteristics of the SFF of the $0 + 1$ SYK model.

On the other hand, if $r_p \gg 1$ i.e.

$$\frac{u}{t} \ll \frac{1}{\sqrt{p}} \tag{83}$$

the dominant term will be $z_2^{(p)}$. Geometrically, this contribution corresponds to connected wormhole configurations. Therefore in this regime the wormhole saddle dominates, and z is non-self-averaging.

In the rest regime of the parameter $\frac{u}{t}$

$$\frac{1}{\sqrt{p}} \lesssim \frac{u}{t} \lesssim p, \tag{84}$$

neither the disk nor the wormhole saddle point dominates. It suggests that there might be a new saddle point that contributes the most. It turns out when our toy model has a well-defined large N limit, the parameters u and t lie in this regime.

---

[5] Recall that $p = N/q$.

We now examine this result more carefully by a saddle point analysis. As we show in the Appendix B, by introducing the G, Σ variable we can rewrite $\langle z \rangle$ as

$$\langle z \rangle = \int_{\mathbb{R}} dG \int_{i\mathbb{R}} \frac{d\Sigma}{2\pi i/N} \Sigma^{N/2} e^{ui^{q/2} \frac{N^{q/2}}{(q/2)!}} G^{q/2} e^{-N\Sigma G}. \quad (85)$$

We again rotate the integral contour as in the model with zero mean

$$\Sigma \to i e^{-i\frac{2\pi}{q}} \sigma, \quad G \to e^{i\frac{2\pi}{q}} g, \quad (86)$$

which leads to the action:

$$\langle z \rangle = \int_{\mathbb{R}} \frac{dg\, d\sigma}{2\pi/N} \exp \left\{ \frac{N}{2} \left(\log(ie^{-\frac{2\pi i}{q}} \sigma) \right. \right.$$
$$\left. \left. - 2i\sigma g - \frac{2\mu}{q} g^{q/2} \right) \right\}, \quad (87)$$

with

$$\mu \equiv i^{q/2} u \frac{2N^{q/2-1}}{(q/2-1)!},$$
$$\leftrightarrow \quad u = (-i)^{q/2} \mu \frac{(q/2-1)!}{2N^{q/2-1}}. \quad (88)$$

The saddle point equations are

$$\frac{1}{\sigma} - 2ig = 0, \quad -2i\sigma - \mu g^{q/2-1} = 0,$$
$$\to \quad \mu g^{q/2} = -1. \quad (89)$$

Comparing (87) with (18) it is easy to find that to reproduce the exact result (76) we have to add the contributions from all the $q/2$ saddles. For the choices (64) and (88) we have

$$\frac{u}{t} \sim \frac{\mu}{\tau} \frac{(q/2-1)!}{\sqrt{(q-1)!}} N^{\frac{1}{2}} \sim \sqrt{p}, \quad (90)$$

which exactly lies in the regime (84). To find the new saddle explicitly, we start from a path integral expression of $\langle z^2 \rangle$

$$\langle z^2 \rangle = \int_R d^3 G_i \int_{i\mathbb{R}} d^3 \Sigma_i \, e^{\frac{N}{q}(\tau^2 G_{LR}^q + \mu G_L^{q/2} + \mu G_R^{q/2}) - N(\Sigma_i G_i)}$$
$$\times \frac{1}{2} \left((\Sigma_{LR} + i\sqrt{\Sigma_L \Sigma_R})^N + (\Sigma_{LR} - i\sqrt{\Sigma_L \Sigma_R})^N \right) \quad (91)$$

whose detailed derivation is in Appendix B. The saddle point equations are

$$G_{L(R)}^{-1+\frac{q}{2}} = \frac{2}{\mu} \Sigma_{L(R)}, \quad G_{LR}^{-1+q} = \frac{1}{\tau^2} \Sigma_{LR}, \quad (92)$$

$$G_{L(R)} = \frac{i\Sigma_{R(L)}}{2\sqrt{\Sigma_L \Sigma_R}} \frac{f_+^{n-1} - f_-^{n-1}}{f_+^n + f_-^n}, \quad (93)$$

$$G_{LR} = \frac{f_+^{n-1} + f_-^{n-1}}{f_+^n + f_-^n}, \quad (94)$$

where $f_{\pm} = \Sigma_{LR} \pm i\sqrt{\Sigma_L \Sigma_R}$. For simplicity, we choose $\tau^2 = \mu = 1$. There are always two types of trivial solutions

wormhole solution : $G_L = G_R = 0,$
$$G_{LR} = e^{\frac{2im\pi}{q}}, \quad (95)$$

disconnect solution : $G_{LR} = 0, \quad G_L = e^{\frac{4im_L\pi}{q}},$
$$G_R = e^{\frac{4im_R\pi}{q}} \quad (96)$$

with on-shell action respectively

wormhole solution : $\langle z^2 \rangle_{\text{wh}} = e^{-N(1-\frac{1}{q})} e^{\frac{2im\pi N}{q}} \quad (97)$

disconnect solution :
$$\langle z^2 \rangle_{\text{dis}} = 2^{-N} e^{-N(1-\frac{2}{q})} e^{\frac{4im\pi N}{q}}. \quad (98)$$

Note that the ratio of these two contributions is

$$\frac{\langle z^2 \rangle_{\text{wh}}}{\langle z^2 \rangle_{\text{dis}}} = \left(2e^{-1/q} \right)^N, \quad (99)$$

so when $q \geq 2$ the wormhole contributes more. We find another solution where only one of $(f_+)^N$ and $(f_-)^N$ survives in the large N limit. Assuming $f_-^N \to 0, N \to \infty$, (94) simplifies to

$$G_{L(R)} = \frac{\Sigma_{R(L)}}{-2i\sqrt{\Sigma_R \Sigma_L}} \frac{1}{\Sigma_{LR} + i\sqrt{\Sigma_L \Sigma_R}}, \quad (100)$$

$$G_{LR} = \frac{1}{\Sigma_{LR} + i\sqrt{\Sigma_L \Sigma_R}}, \quad (101)$$

which leads to

$$G_{LR}^q + G_R^{q/2} + G_L^{q/2} = 1, \quad G_R^{q/2} = G_L^{q/2}. \quad (102)$$

For the case of $q = 4$, (92) and (102) can be solved explicitly and gives the following contribution to the integral (91)

$$\langle z^2 \rangle_{\text{non-trivial}+} \approx e^{-0.63N} e^{\frac{2mi\pi N}{4}}$$
$$> \langle z^2 \rangle_{\text{wh}} = e^{-0.75N} e^{\frac{2mi\pi N}{4}}. \quad (103)$$

We also checked that these solutions indeed satisfies $\lim_{N\to\infty} f_-^N = 0$. There are similar saddles that satisfy $f_+^N = 0$. Therefore we conclude that in the large N limit the dominate saddles are the non-trivial ones.

3.2 The non-self-averaged contributions to z

Contrary to the model with zero means, we expect a non-vanishing "disk" saddle point in this $u \neq 0$ model, which gives $\langle z \rangle \neq 0$, in the path integral representation of z. Moreover, we will show that there are new saddle point contributions to z as shown in Fig. 4, analogous to the half-wormhole contribution to z^2 in the previous model with zero means, which we call the "punctured disk" (or "single half-wormhole") saddles.
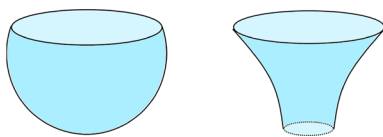
Fig. 4 A pictorial illustration of the "disk" and the "Punctured disk" saddle of z respectively

Fig. 5 Feynman diagrams for $\langle z^2 \rangle$, $\langle \Theta_1^2 \rangle$, $\langle z\Theta_1 \rangle$. Each black dot represents a factor of z, each red dot and the attached line represents a contraction with the J_A^0 source, and each blue line is a contraction of a pair of J_A. So the diagram containing k blue lines corresponds to $z_2^{(k)}$ in (76)

With the help of the collective variables (72), we insert the identity

$$
1 = \int_{-\infty}^{\infty} dG_h \int_{-i\infty}^{i\infty} \frac{N d\Sigma_h}{2\pi i}
$$
$$
\times e^{-\Sigma_h(NG_h - \sum_{i<j} \psi_i\psi_j) + \frac{N\mu}{q}\left(G_h^{q/2} - \left(\frac{1}{N}\sum_{i<j}\psi_i\psi_j\right)^{q/2}\right)}, \quad (104)
$$

into the non-averaged partition function z

$$
z = \int d^N\psi \exp\left(i^{q/2} J_{i_1 \ldots i_q} \psi_{i_1 \ldots i_q}\right). \quad (105)
$$

To make the integral well defined, we again rotate the contour by $\Sigma_h = ie^{-2i\pi/q}\sigma_h$, $G_h = e^{2i\pi/q}g_h$, then z can be cast into the form

$$
z = \int_{-\infty}^{\infty} \frac{N d\sigma_h}{2\pi} \Psi(\sigma_h)\hat{\Theta}(\sigma_h), \quad (106)
$$

where the first factor is similar to (29)

$$
\Psi(\sigma_h) = \int_{\mathbb{R}} \frac{dg_h}{2\pi/N} \exp\left[N\left(-i\sigma_h g_h - \frac{\mu}{q}g_h^{q/2}\right)\right], \quad (107)
$$

and the second factor is

$$
\hat{\Theta}(\sigma_h) = \int d^N\psi \exp\left[ie^{-\frac{2i\pi}{q}}\sigma_h \sum_{i<j}\psi_i\psi_j\right.
$$
$$
\left. + i^{q/2} J_A\psi_A - i^{q/2}u\sum_A \psi_A\right]. \quad (108)
$$

The function $\Psi(\sigma_h)$ is again peaked at $\sigma_h = 0$, so a naive generalization of the proposal of the existence of the half-wormhole saddle suggests the approximation

$$
z \approx \langle z \rangle + \Theta_1, \quad (109)
$$

where

$$
\Theta_1 = \hat{\Theta}(0) = \text{Pf}(J - J^0)
$$
$$
= \sum_A' \text{sgn}(A)(J_{A_1} - J_{A_1}^0)\ldots(J_{A_p} - J_{A_p}^0). \quad (110)
$$

To examine this approximation, we define the error function:

$$
\text{Error} = z - \langle z \rangle - \Theta_1 \quad (111)
$$

and compute variance of the error

$$
\langle \text{Error}^2 \rangle = \langle z^2 \rangle - \langle z \rangle^2 + \langle \Theta_1^2 \rangle - 2\langle z\Theta_1 \rangle. \quad (112)
$$

The quantities $\langle z^2 \rangle$, $\langle \Theta_1^2 \rangle$, $\langle z\Theta_1 \rangle$ can be computed by summing over the Feynman diagrams in Fig. 5.

Recalling that $\langle z^2 \rangle = \sum_{k=0}^{p} z_2^{(k)}$ which is given by summing over all the diagrams, $z_2^{(0)} = \langle z \rangle^2$ which is given by the last diagram in Fig. 5, $z_2^{(p)} = \langle z^2 \rangle_{\mu=0}$ which is given by the first diagram in Fig. 5 and $\langle \Theta_1^2 \rangle = \langle \Theta_1 z \rangle = z_2^{(p)}$, we find

$$
\langle \text{Error}^2 \rangle = \sum_{k=1}^{p-1} z_2^{(k)}. \quad (113)
$$

Based on our analysis in the previous section, this error is negligible only when the ratio of u to t is very small and z exhibits self-averaging, or when the ratio is very large and z is mostly non-self-averaging. However, within the regime defined by inequality (84), the error becomes non-negligible, rendering the naive half-wormhole proposal (109) invalid. The underlying reason for this failure is the emergence of a new saddle point when we tune the parameter u.

One possibility of what is happening in this parameter regime (84) is that a specific Feynman diagram in Fig. 5, denoted as $z_2^{(k)}$, will dominate the summation (76) in the large N limit. If this is the case, it is possible to find a dominant non-self-averaging contribution $\Theta^{(k)}$, which we call the "punctured disk" to z such that

$$
z \approx \langle z \rangle + \Theta^{(k)}, \quad (114)
$$

where the value of k is determined by the value of the parameter u/t.

The non-trivial point is that if this is true, then the approximation of z^2 is in the precise form of the aforementioned proposal

$$
\langle z^2 \rangle \approx z_2^{(k)} + \langle z \rangle^2. \quad (115)
$$

One proposal for the $\Theta^{(k)}$ is

$$
\Theta^{(k)} = \int d^N\psi \frac{(i^{q/2} J_A^{(0)}\psi_A)^{p-k}}{(p-k)!} e^{i^{q/2}(J_B - J_B^{(0)})\psi_B}. \quad (116)
$$

For examples

$$
\Theta^{(p-1)} = \sum_A' \text{sgn}(A)(J_{A_1} - J_{A_1}^0)(J_{A_2} - J_{A_2}^0)\ldots
$$
$$
\ldots J_{A_i}^0 \ldots (J_{A_p} - J_{A_p}^0), \quad (117)
$$

$$\Theta^{(p-2)} = \sideset{}{'}\sum_{A} \mathrm{sgn}(A)(J_{A_1} - J_{A_1}^0) \ldots J_{A_i}^0 \ldots$$

$$\ldots J_{A_j}^0 \ldots (J_{A_p} - J_{A_p}^0),\tag{118}$$

$$\Theta^{(0)} = \langle z \rangle, \quad \Theta^{(p)} = \Theta_1.\tag{119}$$

Then from the Feynman diagrams in Fig. 5 it is not hard to find that

$$\langle \Theta^{(k)} \Theta^{(k)} \rangle = \langle \Theta^{(k)} z \rangle = z_2^{(k)}.\tag{120}$$

This result ensures that (115) is true.

We will present a further analysis from another approach to this model somewhere else.

3.3 The non-self-averaged contributions to z^2

In the previous section, we considered the non-self-averaged contribution $\Theta^{(k)}$ to the partition function z. In this section, we study the non-self-averaged contribution to z^2 and try to understand its relationship with the $z_2^{(k)}$.

The result (114) immediately gives

$$z^2 = \left(\langle z \rangle + \Theta^{(k)} \right)^2 = \langle z \rangle^2 + 2\langle z \rangle \Theta^{(k)} + \left(\Theta^{(k)} \right)^2.\tag{121}$$

In the previous section, we have shown that this relation leads to (115). Using (115), we can further rewrite this relation into

$$z^2 = \langle z^2 \rangle - z_2^{(k)} + 2\langle z \rangle \Theta^{(k)} + \left(\Theta^{(k)} \right)^2.\tag{122}$$

This provides an approximation to z^2

$$z^2 \approx \langle z^2 \rangle + \Lambda^{(k)},\tag{123}$$

where

$$\Lambda^{(k)} = -z_2^{(k)} + 2\langle z \rangle \Theta^{(k)} + \left(\Theta^{(k)} \right)^2\tag{124}$$

We thus observe that once the punctured disk contribution $\Theta^{(k)}$ is known, all the higher boundary non-self-averaging contributions can be recursively determined. Additionally, a geometric interpretation of (124) is that the sum of connected two-boundary contributions, including the wormhole contribution $z_2^{(k)}$ and the linked half-wormhole $\Lambda^{(k)}$ is the same as the sum of all non-self-averaging disconnected contributions, either one disk plus one punctured disk or two punctured disks. This can be shown in Fig. 6.

One might wonder whether $\Lambda^{(k)}$ has a similar expression as the half-wormhole contribution in the model with zero mean that was introduced in [73] and recast in (63). In Appendix C, we demonstrate that this is not the case.
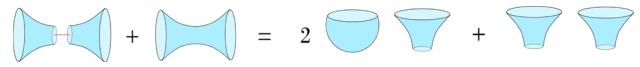
Fig. 6 A pictorial illustration of equation (124)

4 Modified SYK at one time point: beyond Gaussian approximation

The models considered in the literature so far only involve random couplings drawn from Gaussian distributions. On the other hand, SYK-like field theories with other kinds of random couplings are expected to have similar chaotic behaviors as the Gaussian SYK model does. So it is possible that in the low energy limit they also admit effective gravitational descriptions. In particular, explicit examples of field theories with random variables subjecting to other distributions includes the Poisson random variable appearing in the theory of [52,73,82]. Additionally, it is conjectured [22] that any 2-dimensional dilaton gravity theory possesses a dual random matrix description that is generally non-Gaussian. It is therefore interesting to consider random couplings beyond Gaussian distributions and check if there are other non-self-averaging contributions to these models. Separating the physical observables into the self-averaging and non-self-averaging parts is generically applicable in ensemble average theories, so we expect that there always exist half-wormhole-like non-self-averaging saddles for various different observables. We will demonstrate how it works in this section and further understand the relation between the different non-self-averaging quantities.

4.1 SYK at one time point: $\langle J_a \rangle = 0$, $\langle J_a^4 \rangle_c \neq 0$

In this section, we consider theories whose random couplings have vanishing mean values and non-trivial quadrupole moments, namely

$$\langle J_A \rangle = 0, \quad \langle J_A^2 \rangle = t^2, \quad \langle J_A^4 \rangle = v^4 + 3\langle J_A^2 \rangle^2.\tag{125}$$

Note that the introduction of non-vanishing $\langle J_A^4 \rangle - 3\langle J_A^2 \rangle^2$ could potentially alter the outcome of $\langle z^4 \rangle$, but not $\langle z^2 \rangle$. As a result, we expect that the original half-wormhole proposal should be modified. The additional contribution to $\langle z^4 \rangle$ can be attributed to a new wormhole saddle that has four boundaries. In addition, it is reasonable to believe that when $v < t$, this new wormhole saddle is negligible and the original half-wormhole saddle remains valid. We will confirm this through a direct calculation in the following section.

It is easy to compute the correlation functions of the partition function of this model

$$\langle z \rangle = 0, \quad \langle z^2 \rangle = \frac{N!}{p!(q!)^p} t^2.\tag{126}$$

The quadupole moments of J_A in (4.2) contributes nontrivially to $\langle z^4 \rangle$

$$\langle z^4 \rangle = \sum_{A,B,C,D}' \text{sgn}(A)\text{sgn}(B)\text{sgn}(C)\text{sgn}(D)$$
$$\times \langle J_{A_1} J_{B_1} J_{C_1} J_{D_1} \cdots J_{A_p} J_{B_p} J_{C_p} J_{D_p} \rangle, \qquad (127)$$

which can be expanded

$$\langle z^4 \rangle = \sum_{k=0}^{p} c[k] n[N - qk] v^{4k} t^{4(p-k)} \equiv \sum_k z_4^{(k)},$$
$$n[N] = \frac{N!}{(q!)^{2N/q}} \sum_{\substack{n_1+n_2+n_3=N/q \\ n_i \geq 0}} \frac{(qn_1)!(qn_2)!(qn_3)!}{(n_1! n_2! n_3!)^2}, \qquad (128)$$

where $c[k]$ defined in (74) is the number of ways to choose k q-subsets out of N and $n[N]$ is the multiplicities coming from the different Wick contractions. In particular, we get

$$\langle z^4 \rangle_{v=0} = n[N] t^{4p}, \qquad (129)$$

which reduces to the result in [73]. To find the dominant term in the large N limit let us define the ratio

$$\tilde{r}_k = \frac{z_4^{(k)}}{z_4^{(k-1)}} \sim \frac{v^4}{t^4} \frac{1-k+p}{k} \frac{4!(4p-kp)!}{(4p-4k+4)!}, \qquad (130)$$

$$\tilde{r}_1 \sim \frac{v^4}{t^4} \frac{1}{p^2}, \quad \tilde{r}_p \sim \frac{v^4}{t^4} \frac{1}{p}, \qquad (131)$$

where we have again taken $q = 4$ for simplicity. We find that $\tilde{r}_k$ initially decreases and then increases as k increases. For $p > 1$ we have $\tilde{r}_p > \tilde{r}_1$, so $\tilde{r}_p$ is the maximal value. Therefore If $\tilde{r}_p \ll 1$ i.e.

$$\frac{v^4}{t^4} \ll p, \qquad (132)$$

then the dominant term will be $z_4^{(0)}$ and the contributions from non-trivial higher moments, e.g. the nontrivial quadrupole moments proportional to v, can be ignored. Then the situation will be similar to the previous models with $v = 0$. Namely, the half-wormhole saddle of z^2, when $\langle J_A \rangle = 0$, can be written as

$$\Phi = \sum_{A,B}' \text{sgn}(A)\text{sgn}(B) \left(J_{A_1} J_{B_1} - \delta_{A_1 B_1} t^2 \right) \cdots$$
$$\cdots \left(J_{A_p} J_{B_p} - \delta_{A_p B_p} t^2 \right), \qquad (133)$$

such that

$$\langle \Phi^2 \rangle \approx \langle \Phi z^2 \rangle \approx 2\langle z^2 \rangle^2, \qquad (134)$$

and

$$\langle \text{Error}^2 \rangle = \langle z^4 \rangle - \langle z^2 \rangle^2 + \langle \Phi^2 \rangle - 2\langle z^2 \Phi^2 \rangle$$
$$\approx 3\langle z^2 \rangle^2 - \langle z^2 \rangle^2 + 2\langle z^2 \rangle^2 - 4\langle z^2 \rangle^2 = 0, \qquad (135)$$
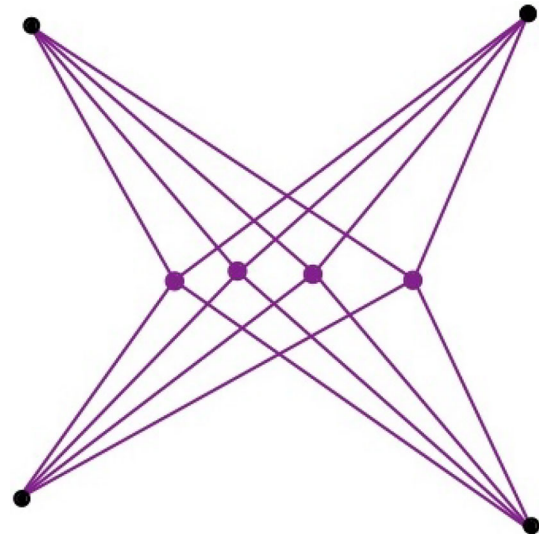
in the leading order of N as before.

Fig. 7 A schematic picture of $z_4^{(p)}$ with $p = 4$, for generic p there are p purple dots in the middle. Each purple line represents a pair of identical J_A's, and the purple dots are vertex coming from the non-trivial quadrupole moment proportional to v

Contrarily, if $\tilde{r}_p \gg 1$, $z_4^{(p)}$ can be the leading contribution, whose corresponding Feynman diagram is shown in Fig. 7.

Therefore, there will be no half-wormhole saddle anymore since the (two-mouth) wormhole saddles are not dominant.

One can consider more general distribution with all the cumulants to be non-vanishing. The analysis and the results will be similar. If v is very large then it is the four-way wormhole saddle that dominate. It is therefore possible to introduce a new "four-linked-half-wormhole" saddle as we show in next section. However, if v is relatively small it is still the two-sided wormhole (with some legs as shown in Fig. 5) that dominates.

4.2 SYK at one time point: $\langle J_a \rangle = \langle J_a^2 \rangle = \langle J_a^3 \rangle = 0$

In this section, we consider a special model where we could focus on the multi-linked half-wormhole saddles. We will show that the multi-linked half-wormhole saddles are not simply related to the two-linked-half-wormhole saddle. In this model the random coupling only have non-vanishing quadrupole moment

$$\langle J_a \rangle = \langle J_a^2 \rangle = \langle J_a^3 \rangle = 0, \quad \langle J_a^4 \rangle = v^4. \qquad (136)$$

Such a distribution could also be considered as an extremal limit of other distributions.

4.2.1 Averaged quantities: $\langle z^4 \rangle$ and $\langle z^8 \rangle$

Due to our special choice (136) the first non-vanishing averaged quantity is

$$
\langle z^4 \rangle = \int \mathrm{d}^{4N}\psi
$$
$$
\times \exp\left(v^4 \sum_{A_1 < \cdots < A_q} \psi^1_{A_1} \psi^2_{A_1} \psi^3_{A_1} \psi^4_{A_1} \cdots \psi^1_{A_q} \psi^2_{A_q} \psi^3_{A_q} \psi^4_{A_q} \right)
$$
$$
= \int \mathrm{d}^{4N}\psi \exp\left(\frac{v^4}{q!} \left(\sum_i^N \psi^1_i \psi^2_i \psi^3_i \psi^4_i \right)^q \right). \tag{137}
$$

Then we can introduce the G, Σ trick

$$
\langle z^4 \rangle = \int \mathrm{d}^{4N}\psi \int \mathrm{d}G
$$
$$
\times \delta\left(G_4 - \sum_i^N \psi^1_i \psi^2_i \psi^3_i \psi^4_i \right) \exp\left(\frac{v^4}{q!} G_4^q \right)
$$
$$
= \int \mathrm{d}^{4N}\psi \int \mathrm{d}G \frac{\mathrm{d}\Sigma}{2\pi\mathrm{i}} \exp\left(-\Sigma\left(G_4 - \sum_i^N \psi^1_i \psi^2_i \psi^3_i \psi^4_i \right) \right)
$$
$$
\times \exp\left(\frac{v^4}{q!} G_4^q \right) = (\partial_{G_4})^N \exp\left(\frac{v^4}{q!} G_4^q \right) |_{G_4=0}
$$
$$
= \left(\frac{v^4}{q!} \right)^{N/q} \frac{N!}{(N/q)!} = v^{4p} \frac{N!}{p!(q!)^p}. \tag{138}
$$

The computation of $\langle z^8 \rangle$ is more involved

$$
\langle z^8 \rangle = \int \mathrm{d}^{8N}\psi \exp\left(\frac{v^4}{q!} \left(\sum_i^N \psi^a_i \psi^b_i \psi^c_i \psi^d_i \right)^q \right), \tag{139}
$$

where

$$
1 \le a < b < c < d \le 8. \tag{140}
$$

In the following we use the collective index A' to label the 4-element string. Introducing antisymmetric tensors $G_{abcd} = G_{A'}$ and $\Sigma_{abcd} = \Sigma_{A'}$ as the collective field variables such that (139) can be expressed as

$$
\langle z^8 \rangle = \int \frac{\mathrm{d}G_{A'}\mathrm{d}\Sigma_{A'}}{(2\pi\mathrm{i})^{70}} (\mathrm{PF}(\Sigma_{A'}))^N
$$
$$
\times \exp\left(-\sum_{A'} \left(\Sigma_{A'} G_{A'} + \frac{v^4}{q!} G_{A'}^q \right) \right) \tag{141}
$$
$$
= \left(\sum_{A'_1 < A'_2}' \mathrm{sgn}(A') \partial_{G_{A'_1}} \partial_{G_{A'_2}} \right)^N \exp\left(\frac{v^4}{q!} G_{A'}^q \right) |_{G_{A'}=0} \tag{142}
$$
$$
\approx \left(\frac{v^4}{q!} \right)^{\frac{2N}{q}} \frac{N!^2}{p!^2} \frac{1}{2} \binom{8}{4} = 35 \left(\frac{v^4}{q!} \right)^{\frac{2N}{q}} \frac{N!^2}{p!^2}, \tag{143}
$$

where in the last line we have taken the large N limit. In this limit we have

$$
\langle z^8 \rangle \approx 35 \langle z^4 \rangle^2. \tag{144}
$$

4.2.2 The un-averaged z^4

Following similar ideas as in the previous sections, we insert a suitable identity to the expression of z^4

$$
z^4 = \int \mathrm{d}^{4N}\psi \exp\left(\mathrm{i}^{q/2} \sum_{A,i} J_A \psi^i_A \right) \int \mathrm{d}G_4
$$
$$
\times \delta\left(G_4 - \sum_i^N \prod_{a=1}^4 \psi^a_i \right)
$$
$$
\times \exp\left(\frac{v^4}{q!} \left[G_4^q - \left(\sum_i^N \prod_{a=1}^4 \psi^a_i \right)^q \right] \right). \tag{145}
$$

Rotating the contour as before we can rewrite z^4 as

$$
z^4 = \int \mathrm{d}\sigma \, \Psi(\sigma) \hat{\Gamma}(\sigma), \tag{146}
$$

where $\Psi(\sigma)$ is same as (29) and the second factor is

$$
\hat{\Gamma}(\sigma) = \int \mathrm{d}^{4N}\psi \exp\left(\mathrm{i}e^{-\frac{\mathrm{i}\pi}{q}} \sigma \prod_a \psi^a_i \right.
$$
$$
\left. + \mathrm{i}^{q/2} \sum_{A,a} J_A \psi^a_A - v^4 \sum_A \prod_a \psi^a_A \right). \tag{147}
$$

Therefore we expect the half-wormhole saddle is given by

$$
\Gamma = \hat{\Gamma}(0)
$$
$$
= \sum_{ABCD} \mathrm{sgn}(A, B, C, D)
$$
$$
\times \prod_{k=1}^p \left(J_{A_k} J_{B_k} J_{C_k} J_{D_k} - \delta^{B_k}_{A_k} \delta^{B_k}_{C_k} \delta^{D_k}_{C_k} v^4 \right), \tag{148}
$$

which satisfies

$$
\langle \Gamma \rangle = 0, \qquad \langle \Gamma^2 \rangle = \langle \Gamma z^4 \rangle \approx 34 \langle z^4 \rangle^2, \tag{149}
$$
$$
\langle (z^4 - \langle z^4 \rangle - \Gamma)^2 \rangle = \langle z^8 \rangle - \langle z^4 \rangle^2 + \langle \Gamma^2 \rangle - 2\langle \Gamma z^4 \rangle
$$
$$
\approx 0. \tag{150}
$$

We find clearly that the contribution from this four-linked-wormhole saddle is not equal to the square of (two-linked) half-wormhole saddle. Even though we derive it in the 0d-SYK toy model, it should exist in other SYK-like theory as long as the G, Σ trick can be applied.

4.3 SYK at one time point: Poisson distribution

Up to now we have only considered random couplings with continuous probability distributions. It is also interesting to consider random couplings that take discrete values such as the Poisson distribution. Ensemble theory or theories with random coupling with Poisson distribution have been studied in [52,59,82]. A property of Poisson distribution is that all the

cumulants are equal; for a model with a $2q$-point interaction among $2N$ fermions, we define

$$\langle J^n \rangle_c = N\lambda, \quad \forall n, \tag{151}$$

so that a large-N limit is well defined. Starting with action (1) we can compute the first few moments

$$\langle z \rangle = \int d^{2N}\psi \, e^{Ni^q\lambda \sum_A \psi_A^1}, \tag{152}$$

$$\langle z^2 \rangle = \int d^{4N}\psi \, e^{Ni^q\lambda \sum_A (\psi_A^1 + \psi_A^2)} e^{Ni^{2q}\lambda \sum_A \psi_A^1 \psi_A^2}, \tag{153}$$

$$\langle z^3 \rangle = \int d^{6N}\psi \, e^{Ni^q\lambda \sum_A (\psi_A^1 + \psi_A^2 + \psi_A^3)}$$
$$\times e^{Ni^{2q}\lambda \sum_A (\psi_A^1 \psi_A^2 + \psi_A^1 \psi_A^3 + \psi_A^2 \psi_A^3)} e^{Ni^{3q}\lambda \sum_A \psi_A^1 \psi_A^2 \psi_A^3}. \tag{154}$$

For a generic k, we find

$$\langle z^k \rangle = \int d^{2kN}\psi \, e^{N\lambda \sum_A \sum_{n=1}^{k} \frac{1}{n!}(i^q \sum_{i=1}^{k}(\psi_A^i))^n}. \tag{155}$$

Formally we can define

$$\mathcal{Z}(\lambda) \equiv \langle z^\infty \rangle \tag{156}$$

$$= \int d\psi \exp\left\{ N\lambda \sum_A \left(e^{i^q \sum_{i=1} \psi_A^i} - 1 \right) \right\}. \tag{157}$$

We can compute these moments by integrating out the fermions directly

$$\langle z^n \rangle = \langle \mathrm{Pf}(J_A)^n \rangle. \tag{158}$$

However, the ensemble average of $\mathrm{PF}(J_A)^n$ in the last expression is very complicated. We therefore look at the large N behavior of $\langle z^n \rangle$, which can be done by introducing G

$$G = \sum_{i<j} i\psi_i \psi_j, \tag{159}$$

and Σ as before and do a saddle point approximation. The G, Σ expression of $\langle z \rangle$ is similar to (B.54)

$$\langle z \rangle = \int d\Sigma dG (-i)^N \Sigma^N e^{Ni^q\lambda \frac{G^q}{q!}} e^{iN\Sigma G}. \tag{160}$$

The saddle point equations are

$$\Sigma G = i, \quad \frac{\lambda}{(q-1)!}(iG)^q = 1, \tag{161}$$

whose solutions are

$$iG = \left(\frac{(q-1)!}{\lambda}\right)^{1/q} e^{\frac{2m\pi i}{q}}, \quad m = 1, \dots, q. \tag{162}$$

The structure of these solutions is identical to that in [73] and the models discussed previously in this paper, so we should

add up all these q saddle points contributions[6]

$$\langle z \rangle_{\mathrm{Disk}} = e^{-N(1-\frac{1}{q})} \left(\frac{N^q\lambda}{(q-1)!}\right)^p \sum_m e^{\frac{2m\pi i}{q}} \tag{163}$$

$$= q e^{-N(1-\frac{1}{q})} \left(\frac{N^q\lambda}{(q-1)!}\right)^p, \tag{164}$$

where $p = N/q$ as before. Adding the 1-loop factor $1/\sqrt{q}$ we end up with the large-N behavior

$$\langle z \rangle_{\mathrm{Disk+1\,loop}} = \frac{1}{\sqrt{q}} e^{-N(1-\frac{1}{q})} \left(\frac{N^q\lambda}{(q-1)!}\right)^p. \tag{165}$$

Other moments can be computed similarly. For example, to compute $\langle z^2 \rangle$, we introduce three collective variables

$$G_1 = \sum_{i<j} i\psi_i^1 \psi_j^1, \quad G_2 = \sum_{i<j} i\psi_i^2 \psi_j^2, \tag{166}$$

$$G_{12} = \sum_i \psi_i^1 \psi_i^2 \tag{167}$$

such that

$$i^q \sum_A \psi_A^1 = \frac{G_1^q}{q!}, \quad i^q \sum_A \psi_A^2 = \frac{G_2^q}{q!}, \tag{168}$$

$$i^{2q} \sum_A \psi_A^1 \psi_A^2 = \frac{G_{12}^{2q}}{(2q)!}. \tag{169}$$

Imposing these relations with the help of a set of Lagrangian multiplier fields Σ_1, Σ_2 and Σ_{12}, the $\langle z^2 \rangle$ can be expressed as

$$\langle z^2 \rangle = \int [d^3 G_i d^3 \Sigma_i] e^{N\frac{\lambda}{q!}(G_1^q + G_2^q + \frac{q!}{(2q)!}G_{12}^{2q})} e^{iN\sum_i(\Sigma_i G_i)}$$
$$\times \int d^{2N}\psi \, e^{\frac{1}{2}\Psi M \Psi}, \tag{170}$$

$$= \int [d^3 G_i d^3 \Sigma_i] \sqrt{\det[\Sigma_1 \Sigma_2 A^2 - \Sigma_{12}^2 I_{2N}]}$$
$$\times e^{\frac{N\lambda}{q!}(G_1^q + G_2^q + \frac{q!}{(2q)!}G_{12}^{2q})} e^{iN\sum_i(\Sigma_i G_i)} \tag{171}$$

$$= \int [d^3 G_i d^3 \Sigma_i] i^{2N} \sum_{k=1}^{N} \binom{2N}{2k} \Sigma_{12}^{2N-2k}(\Sigma_1 \Sigma_2)^k$$
$$\times e^{N\frac{\lambda}{q!}(G_1^q + G_2^q + \frac{q!}{(2q)!}G_{12}^{2q})} e^{Ni\sum_i(\Sigma_i G_i)} \tag{172}$$

where we have defined

$$\Psi = \left(\psi_1^1, \dots, \psi_{2N}^1, \psi_1^2, \dots, \psi_{2N}^2\right), \tag{173}$$

$$M = \begin{pmatrix} \Sigma_1 A & -i\Sigma_{12} I_{2N} \\ i\Sigma_{12} I_{2N} & \Sigma_2 A \end{pmatrix}, \tag{174}$$

$$A = -A^T, \quad A_{ij} = 1, \quad \forall i < j. \tag{175}$$

---

[6] Here we take the large-N limit by considering a series of multiples of 4, so that the normalization factor i^N can be dropped.

The saddle point equations are

$$i\Sigma_i + \frac{\lambda}{(q-1)!}G_i^{q-1} = 0, \quad i = 1, 2, \tag{176}$$

$$i\Sigma_{12} + \frac{\lambda}{(2q-1)!}G_{12}^{2q-1} = 0, \quad \sum_i \Sigma_i G_i = 2i. \tag{177}$$

This set of equations has multiple solutions. For example, the wormhole saddle is

$$G_1 = G_2 = \Sigma_1 = \Sigma_2 = 0, \tag{178}$$

$$G_{12} = \left(\frac{2(2q-1)!}{\lambda}\right)^{1/2q} e^{\frac{2m\pi i}{2q}}, \tag{179}$$

$$\langle z^2 \rangle_{\text{WH+1loop}} = \frac{1}{\sqrt{2q}}e^{-2N(1-\frac{1}{2q})}\left(\frac{(2N)^{2q}\lambda}{2(2q-1)!}\right)^p \tag{180}$$

and the disconnected disk saddle is

$$G_{12} = \Sigma_{12} = 0, \quad G_1 = G_2 = \left(\frac{(q-1)!}{\lambda}\right)^{1/q}, \tag{181}$$

$$\langle z^2 \rangle_{disc+1loop} = \frac{1}{q}e^{-2N(1-\frac{1}{q})}\left(\frac{N^q\lambda}{(q-1)!}\right)^{2p} \tag{182}$$

$$= \langle z \rangle_{\text{Disk+1loop}}^2. \tag{183}$$

The ratio of these two saddles is

$$\frac{\langle z^2 \rangle_{\text{WH+1loop}}}{\langle z^2 \rangle_{\text{Disk+1loop}}} = \sqrt{\frac{q}{2}}\left(\frac{q!^2 2^{2q}}{e\lambda q(2q)!}\right)^p. \tag{184}$$

In the large N or $p = N/q$ limit, the wormhole saddle can dominate only when $\lambda < \frac{q!^2 2^{2q}}{eq(2q)!}\left(\frac{q}{2}\right)^{\frac{1}{2p}}$. For $q = 4$ and $N \to \infty$, this requires $\lambda < 0.336$, which is consistent with what we learned from our previous results. Indeed, for the wormhole or other connected saddle points to be dominant we would like to have non-negligible higher moments of the random coupling. For the Poisson distribution this means, apart from the factors of N to be compensated by powers of fermion contractions, λ should be much larger than λ^2.

Then a natural question is that in this limit how about other n-boundary wormhole saddles? In the following let us focus on a particular n-linked-wormhole saddles. When $n = 2k$ is even, the situation is similar to the one in Sect. 4.2:

$$\langle z^{2k} \rangle_{\text{connected}}$$
$$= \int d^{4kN}\psi dG \frac{d\Sigma}{2\pi} \exp\left(iN\Sigma\left(G - \sum_i \prod_{a=1}^{2k}\psi_i^a\right)\right)$$
$$\times \exp\left(N\frac{\lambda}{(2q)!}G^{2q}\right) \tag{185}$$

$$= \int dG \frac{d\Sigma}{2\pi}(i\Sigma)^{2N}\exp\left(\frac{N\lambda}{(2q)!}G^{2q} + iN\Sigma G\right) \tag{186}$$

where the collective variable G is

$$G = \sum_i \prod_{a=1}^{2k}\psi_i^a. \tag{187}$$

The expression (186) is of the same form as (160) so the saddle point approximation is

$$\langle z^{2k} \rangle_{2k-\text{WH+1loop}} = \langle z^2 \rangle_{2-\text{WH+1loop}} \tag{188}$$

$$= \frac{1}{\sqrt{2q}}e^{-2N(1-\frac{1}{2q})}\left(\frac{(2N)^{2q}\lambda}{2(2q-1)!}\right)^p. \tag{189}$$

When $n = 2k + 1$ is odd, the situation is similar to the one of $n = 1$:

$$\langle z^{2k+1} \rangle_{\text{connected}}$$
$$= \int d^{(4k+2)N}\psi dG \frac{d\Sigma}{2\pi}$$
$$\times \exp\left(iN\Sigma\left(G - \sum_{i<j}\prod_{a=1}^{2k+1}\psi_i^a \prod_{a=1}^{2k+1}\psi_j^a\right)\right)$$
$$\times \exp\left(\frac{N\lambda}{q!}G^q\right) \tag{190}$$

$$= \int dG \frac{d\Sigma}{2\pi}(i\Sigma)^{2N}\exp\left(\frac{N\lambda}{q!}G^q + iN\Sigma G\right), \tag{191}$$

where the collective variable G is obviously defined as

$$G = \sum_{i<j}\prod_{a=1}^{2k+1}\psi_i^a \prod_{a=1}^{2k+1}\psi_j^a, \tag{192}$$

therefore the saddle point approximation is

$$\langle z^{2k+1} \rangle_{(2k+1)-\text{HW+1loop}} = \langle z \rangle_{\text{Disk+1loop}}$$
$$\frac{1}{\sqrt{q}}e^{-N(1-\frac{1}{q})}\left(\frac{N^q\lambda}{(q-1)!}\right)^p. \tag{193}$$

These higher n-linked-wormholes should be compared with the corresponding powers of the disk solution, and furthermore since $\langle z^2 \rangle_{2-\text{WH+1loop}} \gg 1$ and $\langle z^2 \rangle_{\text{Disk+1loop}} \gg 1$ due to large-N so

$$\langle z^{2k} \rangle_{2k-\text{WH+1loop}} \ll \left(\langle z^2 \rangle_{2-\text{WH+1loop}}\right)^k, \tag{194}$$

and

$$\langle z^{2k+1} \rangle_{(2k+1)-\text{WH+1loop}} \ll \left(\langle z \rangle_{\text{Disk+1loop}}\right)^{2k+1}, \tag{195}$$

we conclude that all these multiple-linked wormholes with $k > 0$ are suppressed. In other words, the ensemble of z can be approximated by a Gaussian when the ratio (184) is of order 1.

5 The modified Brownian SYK model

Given the above results in 0 dimension, it is interesting to check if similar stories hold in high-dimensional models. Therefore in this section, we look for the wormhole and half-wormholes saddles in 1d Brownian SYK models [9].

We first briefly review the Brownian SYK model. The Brownian SYK model is characterized by couplings that are only correlated at the same instant of time. Therefore after integrating over the coupling we end up with a local effective action. The quantity that is analogous to the partition function but with some information of real time evolution is

$$
z \equiv \mathrm{Tr}\, U(T)
$$
$$
= \int \mathcal{D}\psi_i \exp\left\{-\mathrm{i}\int_0^T dt \left[-\frac{\mathrm{i}}{2}\psi_i \partial_t \psi_i \right.\right.
$$
$$
\left.\left. + J_{i_1\ldots i_q}(t)\mathrm{i}^{\frac{q}{2}}\psi_{i_1\ldots i_q}\right]\right\}. \tag{196}
$$

The random couplings of this model satisfy

$$
\langle J_A \rangle = 0, \quad \langle J_A(t) J_B(t')\rangle = \delta(t-t')\delta_{AB}\mathcal{J}^2, \tag{197}
$$
$$
\mathcal{J}^2 = 2J\frac{(q-1)!}{N^{q-1}}, \tag{198}
$$

where the one-dimensional Majorana fermions is normalized by

$$
\{\psi_i, \psi_j\} = \delta_{ij}. \tag{199}
$$

In the rest of this section we look for the linked half-wormhole contributions in a generalization of this model.[7] In particular, we consider a generalized Brownian SYK model with non-vanishing mean value of the random couplings:

$$
\langle J_A \rangle = J_A^{(0)} = \mu, \tag{200}
$$
$$
\langle J_A(t) J_B(t')\rangle = \delta(t-t')(\delta_{AB}\tau^2 + \mu^2), \tag{201}
$$

and in this section we use the convention $\{\psi_i, \psi_j\} = 2h\delta_{i,j}$. A comparable model has been examined in [79] with a focus on the half-wormhole saddle. However, the key difference lies in the fact that in [79], the random coupling is expressed as a Grassmann number. In Appendix D, we also revisit this modified the (Brownian) SYK model for comparison purposes with our models.

Taking the disorder averaging of the coupling we obtain the averaged theory

$$
\langle z(T)\rangle_J = \int \mathcal{D}\psi\, e^{-S_a}, \tag{202}
$$
$$
S_a = \frac{1}{2}\int_0^T dt \sum_i^N \psi_i \partial_t \psi_i - \mathrm{i}^{q/2}\int dt \sum_A J_A^{(0)}\psi_A
$$
$$
- \frac{\tau^2}{2}\int dt \left(\sum_A \psi_A^2\right) \tag{203}
$$

[7] A discussion of the linked half-wormhole contributions can be found in the arXiv version [84] of this paper.

We can convert the effective Hamiltonian of the averaged theory as a spin system

$$
\langle z \rangle_J = \mathrm{Tr}\left(e^{-T\mathcal{H}}\right), \tag{204}
$$
$$
\mathcal{H} = -\mathrm{i}^{q/2}\sum_A J_A^{(0)}\psi_A - \frac{\tau^2}{2}\sum_A h^q \tag{205}
$$
$$
= -\mathrm{i}^{q/2}\sum_A J_A^{(0)}\psi_A - \frac{\tau^2}{2}\binom{N}{q}h^q. \tag{206}
$$

When $\mu = 0$, the averaged partition function is given by

$$
\langle z \rangle_J = e^{T\frac{\tau^2}{2}\binom{N}{q}h^q} \equiv 2^N e^{TE_0}, \tag{207}
$$
$$
E_0 = \frac{\tau^2}{2}\binom{N}{q}h^q \sim \frac{\tau^2}{2}N^q h^q. \tag{208}
$$

When $\mu \neq 0$, we have to evaluate the trace

$$
\langle z \rangle_J = e^{TE_0}\mathrm{Tr}(e^{T\mathrm{i}^{q/2}\mu\sum_A\psi_A}) \tag{209}
$$
$$
= e^{TE_0}\int \mathcal{D}^N\psi_i \exp(T\mathrm{i}^{q/2}\sum_i \psi_i). \tag{210}
$$

However there is no simple expression for $\langle z \rangle$. We first consider the simplest case with $q = 1$

$$
I_f = \int \mathcal{D}^N\psi_i \exp(a\sum_i \psi_i). \tag{211}
$$

The idea is to transfer the Majorana fermions to Dirac fermions which have a well-defined rules of integrals. Assuming the total number of fermions is even $N = 2K$ then we introduce K Dirac fermions as

$$
c_i = \frac{1}{2\sqrt{h}}(\psi_{2i-1} - \mathrm{i}\psi_{2i}), \quad c_i^\dagger = \frac{1}{2\sqrt{h}}(\psi_{2i-1} + \mathrm{i}\psi_{2i}),
$$
$$
i = 1, \ldots, K, \tag{212}
$$
$$
\psi_{2i-1} = \sqrt{h}(c_i + c_i^\dagger), \quad \psi_{2i} = \mathrm{i}\sqrt{h}(c_i - c_i^\dagger), \tag{213}
$$

which obey

$$
\{c_i, c_j\} = \{c_i^\dagger, c_j^\dagger\} = 0, \quad \{c_i, c_j^\dagger\} = \delta_{ij} \tag{214}
$$

The integration measure changes as

$$
\mathcal{D}\psi_{2i}\mathcal{D}\psi_{2i-1} = 2h\mathcal{D}c_i\mathcal{D}c_i^\dagger. \tag{215}
$$

Thus the integral can be evaluated as

$$
I_1 = (2h)^K\int \prod_i \mathcal{D}c_i\mathcal{D}c_i^\dagger
$$
$$
\times \exp\left(a\sum_i^K \sqrt{h}\left[(1+\mathrm{i})c_i + (1-\mathrm{i})c_i^\dagger\right]\right) \tag{216}
$$
$$
= (2h)^K\left(2\cosh(\sqrt{2}ah)\right)^K. \tag{217}
$$

Now we let us consider the case of $q = 2$

$$I_2(a) = \int d^N \psi_i \exp\left(\frac{a}{2}\sum_{i\neq j}\psi_i A_{ij}\psi_j\right),$$

with $\quad (A_{ij} = -A_{ij} = a, \quad i < j),$ (218)

which looks like a Gaussian but we need to replace ψ_i with c_i:

$$I_2 = (\sqrt{2h})^N \int \prod_i \mathcal{D}c_i \mathcal{D}c_i^\dagger \, e^{\mathcal{H}}$$ (219)

$$\mathcal{H} = \left(iah\left(\sum_i^K[c_i^\dagger c_i - c_i c_i^\dagger] + 2\sum_{i<j}[c_i c_j - c_i^\dagger c_j^\dagger]\right)\right.$$

$$\left.+2ah\sum_{i<j}[c_i^\dagger c_j + c_i c_j^\dagger]\right)$$ (220)

To get an idea how to compute this integral let us consider a simple case of $N = 4$:

$$\psi_1 = \sqrt{h}(c_1 + c_1^\dagger), \psi_2 = i\sqrt{h}(c_1 - c_1^\dagger),$$
$$\psi_3 = \sqrt{h}(c_2 + c_2^\dagger), \psi_4 = i\sqrt{h}(c_2 - c_2^\dagger),$$ (221)

$$\sum_{i<j}\psi_i\psi_j = ih(c_1^\dagger c_1 - c_1 c_1^\dagger + c_2^\dagger c_2 - c_2 c_2^\dagger + 2c_1 c_2 - 2c_1^\dagger c_2^\dagger)$$

$$+2h(c_1^\dagger c_2 + c_1 c_2^\dagger).$$ (222)

We have four different states $|\Psi_i\rangle$:

$$|00\rangle, \quad c_1^\dagger|00\rangle, \quad c_2^\dagger|00\rangle, \quad c_1^\dagger c_2^\dagger|00\rangle.$$ (223)

So the operator $\sum_{i<j}\psi_i\psi_j$ can be written as a 4×4 matrix:

$$\sum_{i<j}\psi_i\psi_j = \begin{pmatrix} -2ih & 0 & 0 & -2ih \\ 0 & 0 & -2h & 0 \\ 0 & 2h & 0 & 0 \\ -2ih & 0 & 0 & 2ih \end{pmatrix}$$ (224)

with 4 eigenvalues $\{\pm i2h, \pm i2\sqrt{2}h\}$ so path integral over c_i and $c_i^\dagger$ can be computed as

$$\sum_i\langle\Psi_i|e^{a\sum_i\psi_i\psi_j}|\Psi_i\rangle = 2\left(\cos(2ah) + \cos(2\sqrt{2}ah)\right).$$ (225)

For example of $N = 6$, the corresponding matrix is

$$\sum_{i<j}\psi_i\psi_j$$

$$= \begin{pmatrix} -3ih & 0 & 0 & 0 & -2ih & -2ih & -2ih & 0 \\ 0 & -ih & 2h & 2h & 0 & 0 & 0 & -2ih \\ 0 & -2h & -ih & 2h & 0 & 0 & 0 & 2ih \\ 0 & -2h & -2h & -ih & 0 & 0 & 0 & -2ih \\ -2ih & 0 & 0 & 0 & ih & 2h & -2h & 0 \\ -2ih & 0 & 0 & 0 & -2h & ih & 2h & 0 \\ -2ih & 0 & 0 & 0 & 2h & -2h & ih & 0 \\ 0 & -2ih & 2ih & -2ih & 0 & 0 & 0 & 3ih \end{pmatrix}$$ (226)

which can be divided into two blocks. We get the eigenvalues by directly diagonalizing the matrix:

$$\pm 5ih, \quad \pm(2\sqrt{3}+1)ih, \quad \pm 3ih, \quad \pm(2\sqrt{3}-1)ih.$$ (227)

Similarly for general N, we can write effective Hamiltonian defined in (219) as

$$\mathcal{H} = \sum_{i\leq j=1}^k\left(\alpha_{ij}c_i^\dagger c_j + \beta_{ij}c_i c_j^\dagger + \gamma_{ij}c_i^\dagger c_j^\dagger + \theta_{ij}c_i c_j\right),$$ (228)

with

$$\alpha_{ii} = ih, \quad \beta_{ii} = -ih, \quad \alpha_{ij} = 2h, \quad \beta_{ij} = 2h,$$ (229)
$$\gamma_{ij} = -2ih, \quad \theta_{ij} = 2ih, \quad \gamma_{ii} = 0, \quad \theta_{ii} = 0.$$ (230)

This Hamiltonian is quadratic and famously can be diagonalized by the Bogoliubov and Valatin's method [85,86]. Explicitly we can do the transformation by taking an operator basis for the Hamiltonian

$$H = c^\dagger M c$$ (231)

where we have

$$c^\dagger = \left(c_1^\dagger, c_2^\dagger, \ldots, c_1, c_2, \ldots\right).$$ (232)

In the simple case with $N = 4$ the matrix can be expressed as

$$M = \begin{pmatrix} ih & h & 0 & -ih \\ -h & ih & ih & 0 \\ 0 & ih & -ih & h \\ -ih & 0 & -h & -ih \end{pmatrix},$$ (233)

we can directly take the diagonalization and get the eigenvalues

$$i(1 + \sqrt{2})h, \quad -i(1 + \sqrt{2})h,$$ (234)
$$-i(1 - \sqrt{2})h, \quad -i(-1 + \sqrt{2})h.$$ (235)

For simplicity we take the notation as

$$\lambda_1 = i(\sqrt{2} + 1)h, \quad \lambda_2 = i(\sqrt{2} - 1)h,$$ (236)

then the resulting effective Hamiltonian becomes

$$H = \lambda_1 \left(d_1^\dagger d_1 - d_1 d_1^\dagger \right) + \lambda_2 \left(d_2^\dagger d_2 - d_2 d_2^\dagger \right). \tag{237}$$

To evaluate the trace we still take the states as (223) therefore we have

$$\text{Tr}(e^H) = e^{-a(\lambda_1+\lambda_2)} + e^{a(\lambda_1-\lambda_2)} + e^{a(-\lambda_1+\lambda_2)} + e^{a(\lambda_1+\lambda_2)}, \tag{238}$$

so we can recover the result (225). For general N the operator (228) can be expressed as a block matrix

$$M = \begin{pmatrix} A + \mathrm{i}hI_N & -\mathrm{i}A \\ \mathrm{i}A & A - \mathrm{i}hI_N \end{pmatrix}, \tag{239}$$

with

$$A = \begin{pmatrix} 0 & h & h & \cdots \\ -h & 0 & h & \cdots \\ -h & -h & 0 & \cdots \\ \vdots & \vdots & \vdots & \ddots \end{pmatrix} \tag{240}$$

The characteristic equation is

$$\det \left(A + (\mathrm{i}h - \lambda))(A - (\mathrm{i}h + \lambda) - H^2 \right)$$

$$= \det \left((h^2 + \lambda^2)I_N - 2\lambda A \right) \tag{241}$$

$$= (\lambda + h)^N + (\lambda - h)^N = 0. \tag{242}$$

So the eigenvalues are

$$\lambda_m = \mathrm{i}h \tan \left(\frac{m\pi}{2N} \right), \quad m = 1, 3, \ldots, N-1. \tag{243}$$

then the Hamiltonian becomes

$$H = \sum_{i=1}^N \lambda_i \left(d_i^\dagger d_i - d_i d_i^\dagger \right). \tag{244}$$

and the trace will have the form

$$\text{Tr}(e^H) = \sum_{\sigma=\pm 1} e^{a \sum_{i=1}^k \sigma_i \lambda_i} = \sum_\sigma \prod_{i=1}^k e^{a\sigma_i \lambda_i} \tag{245}$$

$$= \prod_{i=1}^k \sum_\sigma e^{a\sigma_i \lambda_i} = 2^k \prod_{i=1}^k \cosh(a\lambda_i), \tag{246}$$

Now let us consider the function

$$X_n = \sum_{1 \le i_1 < \ldots i_n \le N} \psi_{i_1} \ldots \psi_{i_N}. \tag{247}$$

We would like to argue that in the large N limit, we have the approximation

$$n! X_{2n} \approx (X_2)^n, \tag{248}$$

as we find for the 0-dimensional theory. Note that unlike the situation of the 0-dimensional theory, $\{X_n\}$ do not form a basis for X_2^n. For example, let us take $N = 6$, there is indeed the identity

$$X_2^2 = -15 + 2! X_4 \tag{249}$$

but we find that

$$X_2^3 = 3! X_6 + 15 X_2 + 12(\psi_1\psi_2 + \psi_1\psi_6 + \psi_3\psi_4 + \psi_4\psi_5 $$
$$+ \psi_5\psi_6) - 4(\psi_1\psi_4 + \psi_2\psi_4 + \psi_3\psi_6). \tag{250}$$

Let us focus on the second last term in X_2^n

$$X_2^n \approx \ldots c_1 X_{2n-4} + n! X_{2n}, \tag{251}$$

$$c_1 = (n-2)! \binom{n}{2}\binom{N}{2}, \tag{252}$$

where c_1 is computed as follows. We need to pick 2 X_2 out of n and contract them, and the $(n-2)$ X_2's remain not contracted and gives $(n-1)! X_{2n-4}$. Notice that the subleading term is X_{2n-4} instead of X_{2n-2}, since if we contract one fermion in X_2 to get

$$\psi_1\psi_2\psi_1\psi_3 \mapsto \psi_3\psi_2, \tag{253}$$

there is going to be another contraction that gives

$$\psi_1\psi_3\psi_1\psi_2 \mapsto \psi_2\psi_3. \tag{254}$$

The two outcomes simply cancel with each other. The main conclusion of this computation is, given that $X_{2n} \sim N^{2n}$, the subleading terms can be safely neglected and approximate X_{2n} by X_2^n. So in the large N limit, we can use the G, Σ trick to compute the fermionic integral

$$I_q(a) = \int \mathrm{d}^N \psi_i \exp \left(a \sum_A \psi_A \right) \tag{255}$$

$$\approx \int \mathrm{d}^N \psi_i \, e^{a \frac{G^{\frac{q}{2}}}{\frac{q}{2}!}} e^{\mathrm{i}\sigma(G - \sum_{i<j} \psi_i\psi_j)} \mathrm{d}G\mathrm{d}\sigma \tag{256}$$

$$= \int \mathrm{d}G\mathrm{d}\sigma \, I_2(-\mathrm{i}\sigma) e^{a \frac{G^{\frac{q}{2}}}{\frac{q}{2}!}} e^{\mathrm{i}\sigma G} \tag{257}$$

$$= I_2(\mathrm{i}\partial_G) e^{a \frac{G^{\frac{q}{2}}}{\frac{q}{2}!}} |_{G=0}, $$
$$A = \{1 \le a_1 < \cdots < a_q \le N\}. \tag{258}$$

where the function I_2 is defined in (218). We can evaluate this expression and we expect the half-wormhole contributions to be similar as the 0-SYK model

$$z \approx \langle z \rangle + \Theta, \tag{259}$$

$$\Theta = \int \mathrm{d}^N \psi \, e^{-\int_0^T \mathrm{d}t \frac{1}{2} \sum_i^N \psi_i \partial_t \psi_i + \mathrm{i}^{q/2} \int_0^T \mathrm{d}t \sum_A (J_A - \mu)\psi_A}. \tag{260}$$

Indeed we find that in the late time this is a good approximation. The detailed analysis is similar to the Brownian SYK model as we have shown in [84], but it is not particularly illuminating, so we omit them here.

6 Discussion

In this paper we examine the half-wormhole proposal in various simple SYK-like models. We show that the structure of half-wormhole-like non-self-averaging contributions in the 0-dimensional SYK type models depends on the distribution of the couplings. When the distribution of the random couplings admits a non-vanishing mean value, there is a new saddle point, which we call the "punctured disk", to the un-averaged partition function z. When the mean value of the coupling is very large then only the disconnected saddles dominate therefore the correlation functions automatically factorize. On the contrary, when the mean value is not very large compared with the other moments, the wormhole saddles contribute significantly to the path integral. In this case the factorization of spectral correlators can be restored by adding various half-wormhole-like non-self-averaging saddles. Moreover, when the random couplings satisfy a general distribution with non-trivial higher moments, new half-wormhole saddles exist and should be included in the path integral. In models where the random couplings are drawn from discrete distributions, such as the Poisson distribution, we greatly modified the conventional approach of introducing collective variables and provide explicit proposals for the expression of half-wormhole-like contributions.[8] Additionally, we generalize the construction of half-wormhole saddles to the Brownian SYK model and confirm that non-self-averaging saddles also exist and help restore the factorization of the spectral correlators.

There are proposals in [72,74,77,81] of the half-wormhole contributions to z^2 in the original 1d SYK model. It would be interesting to generalize our punctured disk saddle to the SYK model.

Data Availability Statement This manuscript has no associated data or the data will not be deposited. [Authors' comment: This is a theoretical study and there is no experimental data.]

---

8 See [87] for further discussion.

Appendix A: Lefschetz thimbles

In this appendix, we review the method of Lefschetz thimble [83]. Suppose we would like to evaluate the integral

$$Z = \int_{\mathcal{M}_{\mathbb{R}}} \mathrm{d}x^i e^S , \tag{A.1}$$

where the integration contour is $\mathcal{M}_{\mathbb{R}}$. Then we complexify the manifold on which the integration is done to $\mathcal{M}_{\mathbb{C}}$. We choose $\Re(S)$ to be the Morse function, as we want to find the contours where S has a constant imaginary part. The saddle points of the integral are the critical points of the Morse function because of the Cauchy-Riemann equations. Around each critical point on $\mathcal{M}_{\mathbb{C}}$ we introduce a set of local coordinates $\{z_i\}$. The Morse flow is determined by the flow equations

$$\frac{\mathrm{d}z^i}{\mathrm{d}t} = -g^{i\bar{j}}\frac{\partial \bar{S}}{\partial \bar{z}^j}, \quad \frac{\mathrm{d}\bar{z}^j}{\mathrm{d}t} = -g^{i\bar{j}}\frac{\partial S}{\partial z^i} \tag{A.2}$$

where $g^{i\bar{j}}$ is Kähler metric and the bar means complex conjugate. We find

$$\frac{\mathrm{d}(S - \bar{S})}{\mathrm{d}t} = \frac{\partial S}{\partial z^i}\frac{\mathrm{d}z^i}{\mathrm{d}t} - \frac{\partial \bar{S}}{\partial \bar{z}^i}\frac{\mathrm{d}\bar{z}^i}{\mathrm{d}t} = 0, \tag{A.3}$$

which implies that the imaginary part of S is a constant along the flow. Each of the critical points is associated with a pair of flows, the thimble and the anti-thimble. The thimble is the "stable" direction such that the Morse function $\Re(S)$ decays along the thimble and the integral of $\exp(S)$ along the thimble converges. On the contrary, the anti-thimble is the "unstable" direction. Explicitly the boundary conditions for a particular critical point p_σ are

$$\lim_{t \to -\infty} z(t) = p_\sigma, \quad \text{for thimbles}, \tag{A.4}$$

$$\lim_{t \to +\infty} z(t) = p_\sigma, \quad \text{for anti-thimbles}. \tag{A.5}$$

The main statement in [83] that we will use repeatedly is that the integral can be approximated by a weighted sum over

integrals along the thimbles of each critical point

$$Z = \sum_i n_i \int_{\mathcal{J}_i} \mathrm{d}t \, e^{S[t]}, \qquad (A.6)$$

where i runs over all the critical points, $\mathcal{J}_i$ is the Lefschetz thimble attaching to the ith critical point, and the weight n_i is given by the intersection number between the anti-thimble and the original integration contour $\mathcal{M}_{\mathbb{R}}$.

Appendix A.1: some examples

To illustrate how this works, we first go through some simple examples.

Appendix A.1.1: The Gaussian function

Let us consider a simple example with

$$S = -x^2/2 + \sigma x. \qquad (A.7)$$

The integral can be regarded as a zero-dimension theory with quadratic interaction and a complex source σ. The only critical point is at $x = \sigma = a + ib$. The flow equation is

$$\frac{\mathrm{d}x}{\mathrm{d}t} = \bar{x} - (a - ib). \qquad (A.8)$$

Expressing $x = x_1 + ix_2$, we get the following equations

$$\frac{\mathrm{d}x_1}{\mathrm{d}t} = x_1 - a, \quad \frac{\mathrm{d}x_2}{\mathrm{d}t} = b - x_2. \qquad (A.9)$$

The general solution can be easily solved

$$x_1 = a + c_1 e^t, \quad x_2 = b + c_2 e^{-t}, \qquad (A.10)$$

where c_1, c_2 are two undetermined constants. The boundary conditions for the thimble is

$$(x_1, x_2) \to (a, b), \quad t \to -\infty, \qquad (A.11)$$

while for the anti-thimble we have

$$(x_1, x_2) \to (a, b), \quad t \to +\infty, \qquad (A.12)$$

where (a, b) is the critical point. Then with these boundary conditions we can get the equations for the thimble and the anti-thimble respectively

$$x_2 = b, \qquad (A.13)$$
$$x_1 = a. \qquad (A.14)$$

We plot the thimble and the anti-thimble in this case in Fig. 8, where for simplicity we let $\sigma = 1 + \mathrm{i}$.
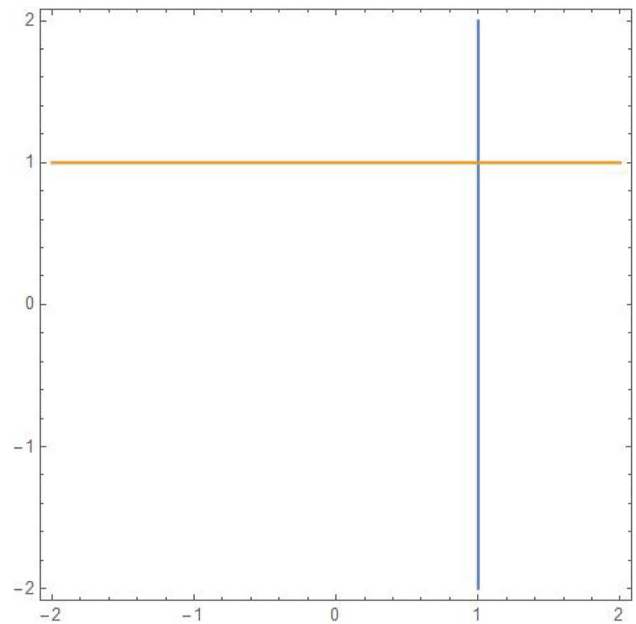
Fig. 8 The red line denotes the thimble and the blue line denotes the anti-thimble. The anti-thimble intersects with the real line, so this saddle point contributes

We can also compare the saddle point solution with the exact result. The integral can evaluated as

$$\int \mathrm{d}x e^{-x^2/2 + \sigma x} = \sqrt{2\pi} e^{\sigma^2/2}. \qquad (A.15)$$

While the saddle point solution gives

$$e^{\sigma^2/2}, \qquad (A.16)$$

with the one-loop correction $\sqrt{2\pi}$ the saddle point analysis recovers the exact result.

A.1.2: The Airy function

A slightly less trivial example is the Airy action

$$Z_\lambda = \int_{-\infty}^{\infty} \mathrm{d}x e^S, \quad S = \mathrm{i}\lambda \left(\frac{x^3}{3} - x \right). \qquad (A.17)$$

It is not hard to find that for real λ there are three "convergent" regions, namely $\Re(S) < \infty$, on the complex x-plane:

$$x = r e^{i\theta}, \quad \frac{2n\pi}{3} \leq \theta \leq \frac{\pi}{3} + \frac{2n\pi}{3}, \quad n = 0, 1, 2. \quad (A.18)$$

In each convergent region, the Airy integrand is exponentially small. As we vary λ to complex values, we should deform the integration contour of x accordingly so that the integral remains converge. This gives an analytic continuation of Z_λ. The two critical points are located at $x = \pm 1$. The values of
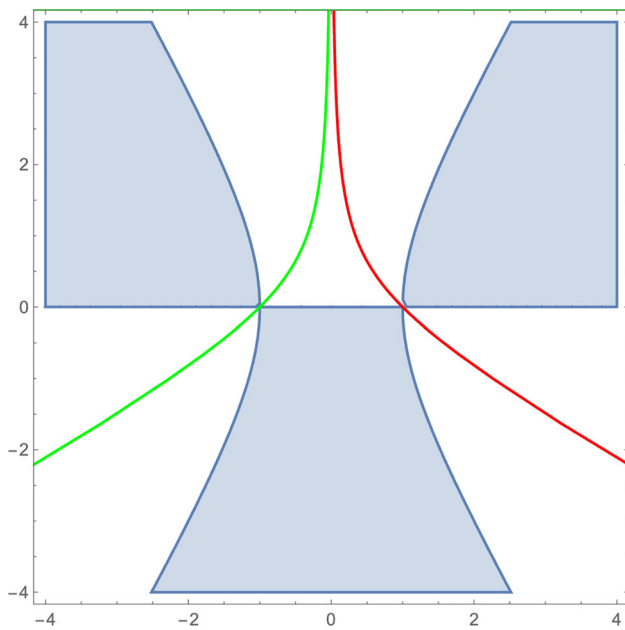
Fig. 9 The red line denotes the anti-thimble of $x = -1$ and the Green line denotes the anti-thimble of $x = 1$. The grey regions are the convergent regions
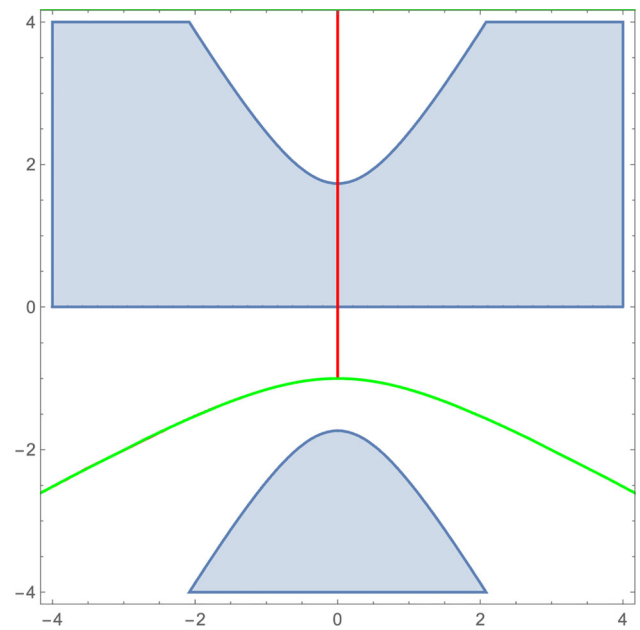

Fig. 10 The red line is the anti-thimble of $x = i$ which intersects with the real line while the Green line is the anti-thimble of $x = -i$ which does not intersect with the real line. The grey regions are the convergent regions

saddle points are

$$S_{\pm} = \mp \frac{2i\lambda}{3}. \tag{A.19}$$

Since along the (anti-)thimbles, the imaginary part of S is a constant and

$$\Im(S_{\pm}) = \mp \frac{2\Re(\lambda)}{3}. \tag{A.20}$$

Therefore the two (anti-)thimbles associated with the two critical points will not intersect except for the case of $\Re(\lambda) = 0$. The thimble which connects critical points is called the Stoke ray. Using the Lefschetz thimbles $\mathcal{J}_{\pm}$, we can rewrite the integral as

$$Z_{\lambda} = n_{+} \int_{\mathcal{J}_{+}} \exp S + n_{-} \int_{\mathcal{J}_{-}} \exp S. \tag{A.21}$$

To solve the thimbles, let us take $\lambda = 1$, then the flow equations are

$$\frac{dx}{dt} = i(\bar{x}^2 - 1). \tag{A.22}$$

Expressing $x = x_1 + ix_2$, we obtain

$$\frac{dx_1}{dt} = 2x_1 x_2, \quad \frac{dx_2}{dt} = x_1^2 - x_2^2 - 1. \tag{A.23}$$

We plot the anti-thimbles in Fig. 9

Therefore for $\lambda = 1$ both of the saddle points contribute. This result is expected since that the two critical points are already located on the real line.

The problem we met in the main text is better illustrated by the following toy model

$$\tilde{Z} = \int_{-\infty}^{\infty} dx \exp S, \quad S = i\left(\frac{x^3}{3} + x\right). \tag{A.24}$$

The integral is convergent and can be expressed by the Airy function

$$\tilde{Z} = \frac{2\pi \operatorname{Ai}\left(\frac{1}{\sqrt[3]{3}}\right)}{\sqrt[3]{3}} = 0.83. \tag{A.25}$$

We now try to compute the integral with saddle point approximation, where the saddle points are located at $x = \pm i$. The saddle point value, plus the 1-loop correction, of the integral at these two saddle points, $\tilde{Z}_{\pm}$ are the same, and the sum of them is larger than the exact evaluation of the integral

$$\tilde{Z}_{+} = \tilde{Z}_{-} = 0.733, \quad \tilde{Z}_{+} + \tilde{Z}_{-} > \tilde{Z}. \tag{A.26}$$

This is exactly the situation we are encountering. In this toy model, it is easy to show that the anti-thimble associated with the saddle point $x = -i$ does not intersect with the real axis, Fig. 10, so the saddle point $x = -i$ does not contribute to the integral.

Appendix A.2: Multi-variable cases

Let us consider another example with two variables

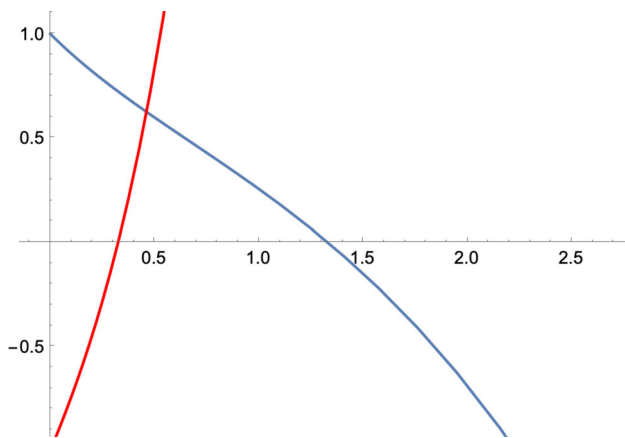$$Z = \int d\sigma \frac{dg}{2\pi} e^S, \quad S = \log \sigma - i\sigma g - \frac{1}{2}g^2. \tag{A.27}$$

Fig. 11 Since $\sigma_\pm$ are already on the real line here we only plot the g-plane of the anti-thimbles. Clearly both of these two anti-thimbles intersect with the real axis so these two saddle points both contribute to the integral

The integral can be done directly to get

$$Z = 0 \,. \tag{A.28}$$

There are two saddle points

$$g_\pm = \pm i, \quad \sigma_\pm = \mp 1. \tag{A.29}$$

with saddle point contributions to the integral (on-shell action)

$$Z_\pm = \mp \frac{1}{\sqrt{e}}, \quad Z_- + Z_+ = 0 \tag{A.30}$$

Matching this with the exact solution suggests that $n_\pm = 1$. Note that $\sigma_\pm = \mp 1$ are already on the real line so corresponding anti-thimbles always intersect with the original contour. The flow equations are

$$\frac{d\sigma}{dt} = -\frac{1}{\bar\sigma} - i\bar g, \quad \frac{dg}{dt} = -i\bar\sigma + \bar g. \tag{A.31}$$

Expressing $\sigma = \sigma_1 + i\sigma_2$ and $g = g_1 + ig_2$ we obtain the following differential equations

$$\frac{d\sigma_1}{dt} + g_2 + \frac{\sigma_1}{\sigma_1^2 + \sigma_2^2} = 0, \tag{A.32}$$

$$\frac{d\sigma_2}{dt} + g_1 + \frac{\sigma_2}{\sigma_1^2 + \sigma_2^2} = 0, \tag{A.33}$$

$$\frac{dg_1}{dt} + \sigma_2 - g_1 = 0, \quad \frac{dg_2}{dt} + \sigma_1 + g_2 = 0. \tag{A.34}$$

We find that indeed these two saddles should both be included. We plot the g-plane of the anti-thimbles in Fig. 11.

Note that this example is special case of (18) with $q = 2$.

• Flow equations in real coordinates

Sometimes it more convenient to use the real form of the flow equations (A.2). We start with the relations

$$\frac{\partial S}{\partial z} = \frac{1}{2}\frac{\partial S}{\partial x} + \frac{1}{2i}\frac{\partial S}{\partial y}, \tag{A.35}$$

$$\frac{\partial \bar S}{\partial \bar z} = \frac{1}{2}\frac{\partial \bar S}{\partial x} - \frac{1}{2i}\frac{\partial \bar S}{\partial y}, \tag{A.36}$$

where

$$z = x + iy. \tag{A.37}$$

Then we evaluate the equation as

$$\frac{dz}{dt} + \frac{d\bar z}{dt} = -\frac{\partial S}{\partial z} - \frac{\partial \bar S}{\partial \bar z} = -\frac{\partial \Re(S)}{\partial x} - \frac{\partial \Im(S)}{\partial y}, \tag{A.38}$$

$$\frac{dz}{dt} - \frac{d\bar z}{dt} = \frac{\partial S}{\partial z} - \frac{\partial \bar S}{\partial \bar z} = -i\frac{\partial \Re(S)}{\partial y} + i\frac{\partial \Im(S)}{\partial x}, \tag{A.39}$$

where we work in the flat space. Recall the Cauchy–Riemann equation we get

$$\frac{dx}{dt} = -\frac{\partial \Re(S)}{\partial x}, \quad \frac{dy}{dt} = -\frac{\partial \Re(S)}{\partial y}. \tag{A.40}$$

To illustrate it we consider a special case in the Airy function

$$S = i\left(\frac{x^3}{3} + x\right). \tag{A.41}$$

In the complex plane its conjugate is

$$\bar S = -i\left(\frac{\bar x^3}{3} + \bar x\right), \tag{A.42}$$

and we can define the components

$$x = x_1 + ix_2, \quad \bar x = x_1 - ix_2. \tag{A.43}$$

The flow equation in complex coordinates becomes

$$\frac{dx}{dt} = -\frac{\partial \bar S}{\partial \bar x} = i(\bar x^2 + 1), \tag{A.44}$$

which leads to the equations in real coordinates

$$\frac{dx_1}{dt} = 2x_1x_2, \quad \frac{dx_2}{dt} = x_1^2 - x_2^2 + 1. \tag{A.45}$$

On the other hand we can get the equations with the real part of S:

$$\Re(S) = -x_2 - x_1^2x_2 + \frac{x_2^3}{3}. \tag{A.46}$$

From the Eqs. (A.40) we can recover the two flow Eq. (A.45).

Appendix B: Details of the derivation of $\langle z \rangle$ and $\langle z^2 \rangle$

This result can be derived by a recursive method with respect to p as shown in [84]. We choose a set of collective variables

$$G = \frac{1}{N} \sum_{1 \leq i < j \leq N} \psi_i \psi_j. \tag{B.47}$$

For simplicity of demonstration let us first consider the $q = 4$ case it is easy to see

$$G^2 = \frac{2!}{N^2} \sum_A \psi_A, \tag{B.48}$$

then $\langle z \rangle$ can be rewritten as

$$\langle z \rangle = \int_{\mathbb{R}} \mathrm{d}G \int_{i\mathbb{R}} \frac{\mathrm{d}\Sigma}{2\pi i/N} \mathrm{d}^N \psi \, e^{-\frac{u}{2} N^2 G^2} e^{-\Sigma(NG - \sum_{i<j} \psi_i \psi_j)}. \tag{B.49}$$

Now we can integrate the out the fermions to get

$$\int \mathrm{d}^N \psi \, e^{\Sigma \sum_{i<j} \psi_i \psi_j} = (\Sigma)^{N/2} m[p]|_{(q=2)} = \Sigma^{N/2}. \tag{B.50}$$

Then (B.49) becomes

$$\langle z \rangle_{q=4} = \int_{\mathbb{R}} \mathrm{d}G \int_{i\mathbb{R}} \frac{\mathrm{d}\Sigma}{2\pi i/N} \Sigma^{N/2} e^{-\frac{uN^2 G^2}{2}} e^{-N\Sigma G}$$

$$= N^{-N/2} (\partial_G)^{N/2} e^{-\frac{uN^2 G^2}{2}} |_{G=0} \tag{B.51}$$

$$= \left(\frac{u}{2}\right)^{N/4} \frac{(N/2)!}{(N/4)!} = m[p] u^p |_{q=4}. \tag{B.52}$$

For general q, the proof is similar with the modification

$$\sum_A \psi_A = \frac{N^{q/2}}{(q/2)!} G^{q/2}. \tag{B.53}$$

In summary, we have generalized the G, Σ trick and derived an effective action to compute $\langle z \rangle$:

$$\langle z \rangle = \int_{\mathbb{R}} \mathrm{d}G \int_{i\mathbb{R}} \frac{\mathrm{d}\Sigma}{2\pi i/N} \Sigma^{N/2} e^{u i^{q/2} \frac{N q/2}{(q/2)!} G^{q/2}} e^{-N\Sigma G}. \tag{B.54}$$

By introducing the following collective variables

$$G_{LR} = \frac{1}{N} \sum_i \psi_i^L \psi_i^R, \tag{B.55}$$

$$G_L = \frac{1}{N} \sum_{i<j} \psi_i^L \psi_j^L, \quad G_R = \frac{1}{N} \sum_{i<j} \psi_i^R \psi_j^R, \tag{B.56}$$

the averaged quantity $\langle z^2 \rangle$ can be expressed as

$$\langle z^2 \rangle = \int_R \mathrm{d}^3 G_i \int_{i\mathbb{R}} \mathrm{d}^3 \Sigma_i \, e^{\frac{N}{q}(\tau^2 G_{LR}^q + \mu G_L^{q/2} + \mu G_R^{q/2}) - N(\Sigma_i G_i)}$$

$$\times \int \mathrm{d}^{2N} \psi \, e^{\frac{1}{2} \Psi M \Psi}, \tag{B.57}$$

$$= \int_R \mathrm{d}^3 G_i \int_{i\mathbb{R}} \mathrm{d}^3 \Sigma_i \, e^{\frac{N}{q}(\tau^2 G_{LR}^q + \mu G_L^{q/2} + \mu G_R^{q/2}) - N(\Sigma_i G_i)}$$

$$\times \sqrt{\det[\Sigma_L \Sigma_R A^2 + \Sigma_{LR}^2]}, \tag{B.58}$$

$$= \int_R \mathrm{d}^3 G_i \int_{i\mathbb{R}} \mathrm{d}^3 \Sigma_i \sum_{m=0}^{N/2} \binom{N}{2m} (\Sigma_{LR})^{2m}$$

$$\times (i^2 \Sigma_L \Sigma_R)^{\frac{N}{2} - m} e^{\frac{N}{q}(\tau^2 G_{LR}^q + \mu G_L^{q/2} + \mu G_R^{q/2})} e^{-N(\Sigma_i G_i)}, \tag{B.59}$$

where we have defined

$$\Psi = \left(\psi_1^L, \ldots, \psi_N^L, \psi_1^R, \ldots, \psi_N^R\right), \tag{B.60}$$

$$M = \begin{pmatrix} \Sigma_L A & \Sigma_{LR} I_N \\ -\Sigma_{LR} I_N & \Sigma_R A \end{pmatrix}, \tag{B.61}$$

$$A = -A^T, \quad A_{ij} = 1, \quad \forall i < j. \tag{B.62}$$

Using the same tricks of integration by part, it can be evaluated exactly as

$$\langle z^2 \rangle = N^{-N} \sum_{k=0}^p \binom{N}{kq} (\partial_{G_{LR}})^{kq} (i^2 \partial_{G_L} \partial_{G_R})^{\frac{N-kq}{2}}$$

$$\times e^{\frac{N}{q}(\tau^2 G_{LR}^q + \mu G_L^{q/2} + \mu G_R^{q/2})} |_{G_i=0} \tag{B.63}$$

$$= N^{-N} \sum_{k=0}^p i^{N-kq} \binom{N}{kq} \frac{(kq)!}{k!} \left(\frac{N\tau^2}{q}\right)^k \left[\frac{(\frac{q(p-k)}{2})!}{(p-k)!}\right]^2$$

$$\times \left(\frac{N\mu}{q}\right)^{2p-2k} \tag{B.64}$$

$$= \sum_{k=0}^p c_k m_{p-k}^2 t^{2k} u^{2p-2k}, \tag{B.65}$$

where $m[p]$ is defined in (68) and the coefficient $c[k]$ is

$$c[k] = \frac{N!}{k!(q!)^k (N-kq)!}. \tag{B.66}$$

Appendix C: A naive expression of the half-wormhole contribution and its failure

Inspired by our analysis of the punctured disks for z, we can insert another two copies of identities (104) in z^2

$$z^2 = \int \mathrm{d}\sigma_w \mathrm{d}\sigma_{h_L} \mathrm{d}\sigma_{h_R} \Psi(\sigma_w, \sigma_{h_L}, \sigma_{h_L}) \hat{\Lambda}(\sigma_w, \sigma_{h_L}, \sigma_{h_L}), \tag{C.67}$$

$$\Psi(\sigma_w, \sigma_{h_L}, \sigma_{h_L}) = \Psi(\sigma_w) \Psi(\sigma_{h_L}) \Psi(\sigma_{h_R}), \tag{C.68}$$

$$\hat{\Lambda}(\sigma_w, \sigma_{h_L}, \sigma_{h_L})$$

$$= \int \mathrm{d}^{2N}\psi \exp\left[\mathrm{i}e^{-\frac{2\mathrm{i}\pi}{q}}\sigma_{h_L}\sum_{i<j}\psi_{ij}^L + \mathrm{i}e^{-\frac{2\mathrm{i}\pi}{q}}\sigma_{h_R}\sum_{i<j}\psi_{ij}^R \right.$$
$$+\mathrm{i}e^{\frac{\mathrm{i}\pi}{q}}\sigma_w\psi_i^L\psi_i^R + \mathrm{i}^{q/2}J_A(\psi_A^L + \psi_A^R)$$
$$\left. -\mathrm{i}^{q/2}u\sum_A(\psi_A^L + \psi_A^R) - \mathrm{i}^q t^2\psi_A^L\psi_A^R \right], \qquad (\text{C.69})$$

where we have introduced three pairs of G, Σ variables

$$G_w = \frac{1}{N}\psi_i^L\psi_i^R, \qquad (\text{C.70})$$

$$G_{h_L} = \frac{1}{N}\sum_{i<j}\psi_{ij}^L, \quad G_{h_R} = \frac{1}{N}\sum_{i<j}\psi_{ij}^R, \qquad (\text{C.71})$$

and rotated the contour as before. As before, the function Ψ is highly peaked around $\Psi(0,0,0)$ so one may expect that there is a half-wormhole saddle point

$$\Lambda = \hat{\Lambda}(0,0,0)$$
$$= \sum_{A,B}^{'}\mathrm{sgn}(A)\mathrm{sgn}(B)$$
$$\times \prod_{k=1}^p \left((J_{A_k} - J_{A_k}^0)(J_{B_k} - J_{B_k}^0) - \delta_{A_k B_k}t^2 \right), \quad (\text{C.72})$$

whose average manifestly vanishes $\langle\Lambda\rangle = 0$ and it further satisfies $\langle\Lambda^2\rangle = \langle z^2\Lambda\rangle = 2z_2^{(p)2}$. If we naively follow the discussion in [73] and propose the following approximation

$$z^2 \approx \langle z^2\rangle + \Lambda \qquad (\text{C.73})$$

then the error can be evaluated as

$$\left\langle \left(z^2 - (\langle z^2\rangle + \Lambda)\right)^2 \right\rangle = \langle z^4\rangle - \langle z^2\rangle^2 - 2\langle z^2\Lambda\rangle + \langle\Lambda^2\rangle$$
$$> 2\langle z^2\rangle^2 - 2z_2^{(p)2} \approx 2(z_2^{(k)})^2, \qquad (\text{C.74})$$

where we have used

$$\langle z^4\rangle > 3\langle z^2\rangle^2, \quad \langle z^2\rangle \approx z_2^{(k)}. \qquad (\text{C.75})$$

Therefore, the average of the error square and $\langle z^2\rangle^2$ are in the same order in the large N limit, which meaning the approximation (C.73) is not accurate.

Appendix D: Random coupling from product of Grassmann variables $J_A^{(0)} = J\prod_i \theta_{A_i}$

A modified SYK-like model dubbed as partially disorder-averaged SYK model is proposed in [81]. In this model, the random coupling $\widetilde{J}_A$ consists of two pieces

$$\widetilde{J}_A = J_A + J_A^{(0)} \qquad (\text{D.76})$$

where J_A is the standard random coupling of the SYK model while $J_A^{(0)}$ is specially chosen as

$$J_{i_i\ldots i_q}^{(0)} = \mathrm{i}^{q/2}q!\mu\,\theta_{i_1}\ldots\theta_{i_q}, \quad \text{with} \quad \{\theta_i, \theta_j\} = 2\delta_{ij} \quad (\text{D.77})$$

so we can think of it as coupling the fermions ψ_i in the original model with some background Majorana fermions θ_i (or non-dynamical fermions living in another universe [81]). Note that $J_A^{(0)}$ is not a c-number which is different from our models studied in the previous section.

D.0.1: 0d model

Let us first consider the 0-dimensional model to see the difference explicitly. In this case the integral (1) can be written as

$$z = \int \mathrm{d}^N\psi \exp\left(\mathrm{i}^{q/2}\sum \widetilde{J}_{i_1\ldots i_q}\psi_{i_1\ldots i_q} \right)$$
$$= \int \mathrm{d}^N\psi \exp\left(\mathrm{i}^{q/2}\sum_A J_A\psi_A + \mu\left(\sum_i \theta_i\psi_i\right)^q \right). \qquad (\text{D.78})$$

The averaged quantity $\langle z\rangle$

$$\langle z\rangle = \int \mathrm{d}^N\psi \exp\left(\mu\left(\sum_i \theta_i\psi_i\right)^q \right), \qquad (\text{D.79})$$

can be computed in two ways. One can integrate out the fermions ψ_i directly. The result is

$$\langle z\rangle = \frac{\mu^{N/q}N!}{(N/q)!}\int \mathrm{d}^N\psi\,(\theta_1\psi_1)\ldots(\theta_N\psi_N) \qquad (\text{D.80})$$

$$= \left[\prod_i \theta_i\right]\frac{\mu^{N/q}N!}{(N/q)!} \equiv \left[\prod_i \theta_i\right]\mathfrak{m}_p. \qquad (\text{D.81})$$

Note that z is not a c-number and depends on the background fermions living in other universe. Here we will not think of this as a problem but a feature since the model is not exactly the original SYK model. Alternatively we can compute this average quantity by the G, Σ trick:

$$G_\sigma = \sum_i \theta_i\psi_i,$$

$$\langle z\rangle = \int \mathrm{d}^N\psi \int \mathrm{d}G_\sigma\frac{\mathrm{d}\Sigma_\sigma}{2\pi}e^{\mathrm{i}[\Sigma_\sigma(G_\sigma - \sum_i \theta_i\psi_i)]}e^{\mu G_\sigma^q}$$

$$= \left[\prod_i \theta_i\right]\int \mathrm{d}G_\sigma\frac{\mathrm{d}\Sigma_\sigma}{2\pi}\Sigma_\sigma^N e^{\mathrm{i}\Sigma_\sigma G_\sigma + \mu G_\sigma^q} \qquad (\text{D.82})$$

$$= \left[\prod_i \theta_i\right](\partial_{G_\sigma})^N e^{\mu G_\sigma^q}|_{G_\sigma=0} \qquad (\text{D.83})$$

$$= \left[\prod_i \theta_i\right]\frac{\mu^{N/q}N!}{(N/q)!}. \qquad (\text{D.84})$$

One can also use the effective action (D.82) to derive the large N result of (D.79) as shown in [81]. We will not repeat that analysis here. Instead, we would like to consider the half-wormhole saddle of z

$$z \approx \langle z \rangle + \Theta \qquad (D.85)$$

as we did in last section. The subtlety is that as we stressed z is not a c-number so the approximation (D.85) is in the sense

$$\langle [z - (\langle z \rangle + \Theta)]^2 \rangle \approx 0, \qquad (D.86)$$

which is a c-number due to (D.77) is small. Let us proceed by computing the averaged quantity $\langle z^2 \rangle$

$$\langle z^2 \rangle = \int d^{2N}\psi \exp\left(\frac{\tau^2}{q!} \left(\sum_i \psi_i^L \psi_i^R \right)^q \right.$$
$$\left. + \mu \left(\sum_i \theta_i \psi_i^L \right)^q + \mu \left(\sum_i \theta_i \psi_i^R \right)^q \right), \qquad (D.87)$$

$$= \int d^{2N}\psi \sum_k \left(\frac{\tau^2}{q!} \right)^k$$
$$\times \sum_{i_1 < \cdots < i_{kq}} (\psi_{i_1}^{LR} \dots \psi_{i_{qk}}^{LR}) \frac{(qk)!}{k!} \left(\frac{(N-kq)!}{(N/q-k)!} \right)^2 \mu^{2p-2k}$$
$$\times \sum_{j_1 < \cdots < j_{N-qk} \neq \{i\}} (\theta_{j_1} \psi_{j_1}^L) \dots (\theta_{j_{N-qk}} \psi_{j_{N-kq}}^L)(\theta_{j_1} \psi_{j_1}^R)$$
$$\dots (\theta_{j_{N-k}} \psi_{j_{N-kq}}^R), \qquad (D.88)$$

$$= \int d^{2N}\psi \sum_k \left(\frac{\tau^2}{q!} \right)^k \mu^{2p-2k} \frac{(qk)!}{k!} \left(\frac{(N-kq)!}{(N/q-k)!} \right)^2$$
$$\times \binom{N}{kq} \psi_1^{LR} \dots \psi_N^{LR}, \qquad (D.89)$$

$$= \sum_k \left(\frac{\tau^2}{q!} \right)^k \mu^{2p-2k} \frac{(qk)!}{k!} \left(\frac{(N-kq)!}{(N/q-k)!} \right)^2 \binom{N}{kq}, \quad (D.90)$$

$$= \sum_k^p \tau^{2k} \mu^{2(p-k)} c_k \mathfrak{m}_{p-k}^2 \equiv \sum_k \mathfrak{z}_2^{(k)}, \qquad (D.91)$$

where c_k of defined in (74) and $\mathfrak{m}_p$ is defined in (D.81). The result (D.87) is in the same form of (B.65). So the analysis of the half-wormhole saddle will be similar; we insert the a suitable identity to (D.78)

$$z = \int d^N\psi \exp\left(i^{q/2} \sum \widetilde{J}_{i_1 \dots i_q} \psi_{i_1 \dots i_q} \right) \int dG_\sigma$$
$$\times \delta \left(G_\sigma - \sum_i \theta_i \psi_i \right) \exp\left(\frac{\mu}{q!} \left(G_\sigma^q - \left(\sum_i \theta_i \psi_i \right)^q \right) \right), \qquad (D.92)$$

$$= \int d^N\psi \frac{d\Sigma_\sigma dG_\sigma}{2\pi i} \exp\left(i^{q/2} \sum_A J_A \psi_A + \Sigma_\sigma \sum_i \theta_i \psi_i \right)$$
$$\times \exp\left(-\Sigma_\sigma G_\sigma + \frac{\mu}{q!} G_\sigma^q \right). \qquad (D.93)$$

Following the arguments below (104) one can obtain the half-wormhole saddle[9]

$$\Theta = \left[\prod_i \theta_i \right] \int d^N\psi \exp\left(i^{q/2} \sum_A J_A \psi_A \right). \qquad (D.94)$$

Then it is easy to find that the half-wormhole saddle satisfies

$$\langle \Theta \rangle = 0, \quad \langle \Theta^2 \rangle = \langle \Theta z \rangle = \mathfrak{z}_2^{(p)}, \qquad (D.95)$$

so the approximation (D.85) will be sufficient if $\mathfrak{z}_2^{(p)}$ is the dominant term in (D.91) as we have shown in last section. When $\mathfrak{z}_2^{(p)}$ is not the dominant term we have to consider the contribution of fluctuation of Σ_σ. To finish our analysis of the half-wormhole saddle for z, let us redo the computation of $\langle z^2 \rangle$ with the G, Σ trick. We need introduce three G variables

$$G_{LR} = \frac{1}{N} \sum_i \psi_i^L \psi_i^R, \qquad (D.96)$$

$$G_L = \frac{1}{N} \sum_i \theta_i \psi_i^L, \quad G_R = \frac{1}{N} \sum_i \theta_i \psi_i^R \qquad (D.97)$$

then $\langle z^2 \rangle$ can be written as

$$\langle z^2 \rangle = \int d^{2N}\psi \prod_a dG_a \prod_a \frac{d\Sigma_a}{2\pi i/N}$$
$$\times \exp\left(\frac{N}{q} \left(tG_{LR}^q + uG_L^q + uG_R^q \right) \right)$$
$$\times \int \exp\left(-\Sigma_{LR} \left(NG_{LR} - \sum_i \psi_i^L \psi_i^R \right) \right)$$
$$\times \exp\left(-\Sigma_L \left(NG_L - \sum_i \theta_i \psi_i^L \right) \right)$$
$$\times \exp\left(-\Sigma_R \left(NG_R - \sum_i \theta_i \psi_i^R \right) \right), \qquad (D.98)$$

$$= \int \left[\prod_a dG_a \frac{d\Sigma_a}{2\pi i/N} \right]$$
$$\times \exp\left(N \left(\frac{t}{q} G_{LR}^q + \frac{u}{q} G_L^q + \frac{u}{q} G_R^q - \sum_a \Sigma_a G_a \right) \right)$$
$$\times (\Sigma_{LR} + \Sigma_L \Sigma_R)^N, \qquad (D.99)$$

where in order to have a well-defined large N scaling we have introduced

$$t = \frac{\tau^2}{(q-1)!} N^{q-1}, \quad u = q\mu N^{q-1}. \qquad (D.100)$$

The saddle point equations are

$$tG_{LR}^{q-1} = \Sigma_{LR}, \quad uG_L^{q-1} = \Sigma_L, \quad uG_R^{q-1} = \Sigma_R, \qquad (D.101)$$

$$G_{LR} = \frac{1}{\Sigma_{LR} + \Sigma_L \Sigma_R}, \quad G_L = -\frac{\Sigma_R}{\Sigma_{LR} + \Sigma_L \Sigma_R}, \qquad (D.102)$$

---

[9] Here the factor $\prod_i \theta_i$ should be present.

$$G_R = -\frac{\Sigma_L}{\Sigma_{LR} + \Sigma_L \Sigma_R} . \tag{D.103}$$

The obvious solutions are the "wormhole" saddles with

$$G_L = G_R = \Sigma_L = \Sigma_R = 0, \tag{D.104}$$

which corresponds to $\mathfrak{z}_2^p$. There are also other saddles corresponding to other $\mathfrak{z}_2^k$. For the simplest case $q = 2$, these solutions can be written explicitly. The "wormhole" saddles are

$$G_L = G_R = \Sigma_L = \Sigma_R = 0, \tag{D.105}$$

$$G_{LR} = \pm\frac{1}{\sqrt{t}}, \quad \Sigma_{LR} = \pm\sqrt{t}, \tag{D.106}$$

$$\langle z^2 \rangle_{\text{WH}} = e^{-\frac{N}{2}} t^{N/2}, \tag{D.107}$$

which do not depend on μ and the other four solutions are

$$\Sigma_L = \Sigma_R = uG_L = uG_R = \pm\sqrt{\frac{u^2 - t}{u}}, \tag{D.108}$$

$$\Sigma_{LR} = \frac{t}{u}, \quad G_{LR} = \frac{1}{u} \tag{D.109}$$

$$\Sigma_L = uG_L = -\Sigma_R = -uG_R = \pm\sqrt{\frac{u^2 - t}{u}}, \tag{D.110}$$

$$\Sigma_{LR} = -\frac{t}{u}, \quad G_{LR} = -\frac{1}{u}, \tag{D.111}$$

$$\langle z^2 \rangle_{\text{new}} = e^{-\frac{N}{2}(2-\frac{t}{u^2})} u^N \tag{D.112}$$

Apparently when $u \to \infty$, $\Sigma_{LR}, G_{LR} \to 0$, then we expect that in this limit the dominant saddle will correspond to $\mathfrak{z}_2^0$ since in this limit saddle point value does not depend on t. Comparing these two saddle values we find

$$\frac{\langle z^2 \rangle_{\text{WH}}}{\langle z^2 \rangle_{\text{new}}} = \exp\left(\frac{N}{2}(1 - x + \log x)\right) \le 1, \tag{D.113}$$

$$x = \frac{t}{u^2} . \tag{D.114}$$

Note that when $x = 1$ such that $\langle z^2 \rangle_{\text{WH}} = \langle z^2 \rangle_{\text{new}}$ the new saddle just reduces to the wormhole saddle. Therefore it implies that the new saddle always dominates.

This new saddle is named as "unlinked half-wormhole" in [81] to distinguish it from the half-wormhole saddle which was found in [73]. One interpretation of this new saddle is that it is the analogue of the disconnected saddle in this model; indeed, we do not find other disconnected saddle with $G_{LR} = 0$, $\Sigma_{LR} = 0$ and $G_{L/R}, \Sigma_{L/R} \ne 0$, in addition, this saddle is present only when $u \ne 0$, and this saddle is more and more important as u increases.

The analysis of the half-wormhole saddle for z^2 will be similar so we will not repeat here.

D.0.2: 1d model

Now we come back to the 0+1d model that is a variant of the Brownian SYK model. Let us begin by deriving the wormhole saddle of $\langle z^2 \rangle$[10]

$$z_L z_R = \int d^{2N}\psi \exp\left\{-\int_0^T dt \frac{1}{2}\sum_i \left(\psi_i^L \partial_t \psi_i^L + \psi_i^R \partial_t \psi_i^R\right)\right.$$
$$\left. + i^{q/2} \int_0^T dt \sum_A \tilde{J}_A \left(\psi_A^L + \psi_A^R\right)\right\} \tag{D.115}$$

$$\langle z_L z_R \rangle$$
$$= \int d^{2N}\psi \exp\left\{-\int_0^T dt \frac{1}{2}\sum_i (\psi_i^L \partial_t \psi_i^L + \psi_i^R \partial_t \psi_i^R)\right.$$
$$+ \int_0^T dt \left(\frac{\tau^2}{q!}\left(\sum_i \psi_i^L \psi_i^R\right)^q + \mu\left(\sum_i \theta_i \psi_i^L\right)^q\right.$$
$$\left.+ \mu\left(\sum_i \theta_i \psi_i^R\right)^q\right) + \tau^2 E_0 T\right\} . \tag{D.116}$$

$$= \int d^{2N}\psi \left[\prod_a dG_a \frac{d\Sigma_a}{2\pi i}\right] \exp\left\{-\int_0^T dt \frac{1}{2}\sum_i (\psi_i^L \partial_t \psi_i^L \right.$$
$$+ \psi_i^R \partial_t \psi_i^R) + \tau^2 T E_0 + \int_0^T dt \left(\frac{\tau^2}{q!}G_{LR}^q + \mu G_L^q\right.$$
$$+ \mu G_R^q - \sum_a \Sigma_a G_a + \sum_i \left[\Sigma_{LR}\psi_i^L \psi_i^R + \Sigma_L \theta_i \psi_i^L\right.$$
$$\left.\left.+ \Sigma_R \theta_i \psi_i^R\right]\right)\right\}, \tag{D.117}$$

where $E_0 = \binom{N}{q}$ is the constant term coming from $\psi_A^{L(R)}\psi_A^{L(R)} = (-1)^{\frac{q}{2}}$. As explained in [73], we can focus on the time-independent saddles then the fermions can be simply integrated out. The result is[11]

$$\langle z_L z_R \rangle$$
$$= e^{T\tau^2 E_0} \int \left[\prod_a dG_a \frac{d\Sigma_a}{2\pi i}\right] e^{TN(\frac{t}{q}G_{LR}^q + \frac{u}{q}G_L^q + \frac{u}{q}G_R^q - \sum_a \Sigma_a G_a)}$$
$$\times \left[\cosh\left(T\sqrt{\Sigma_L^2 + \Sigma_R^2 - \Sigma_{LR}^2}\right)\right]^N .$$
$$= \int \left[\prod_a dG_a \frac{d\Sigma_a}{2\pi i}\right] e^{\tau^2 T E_0} e^{S_{eff}} \tag{D.118}$$

For general T, the saddle equation is very hard to solve due to the complexity of cosh function. However the equations simplify in the large T limit because of the following approximations

$$\log\left(\cosh\left(T\sqrt{\Sigma_L^2 + \Sigma_R^2 - \Sigma_{LR}^2}\right)\right)$$
$$\approx \pm iT\sqrt{\Sigma_{LR}^2 - \Sigma_L^2 - \Sigma_R^2} . \tag{D.119}$$

---

[10] Here we have assumed the large N limit, the exact treatment can be found in [73]

[11] This is result is different from the one derived in [81]. It seems that they used a wrong formula for the fermion integral.

Then in this limit the effective action becomes

$$S_{eff} = TN\left(\frac{t}{q}G_{LR}^q + \frac{u}{q}G_L^q + \frac{u}{q}G_R^q - \sum_a \Sigma_a G_a\right)$$
$$\pm iNT\sqrt{\Sigma_{LR}^2 - \Sigma_L^2 - \Sigma_R^2}, \qquad (D.120)$$

and corresponding saddle point equations are

$$tG_{LR}^{q-1} = \Sigma_{LR}, \qquad (D.121)$$

$$uG_L^{q-1} = \Sigma_L, \quad uG_R^{q-1} = \Sigma_R, \qquad (D.122)$$

$$G_{LR} = \pm\frac{i\Sigma_{LR}}{\sqrt{\Sigma_{LR}^2 - \Sigma_L^2 - \Sigma_R^2}}, \qquad (D.123)$$

$$G_L = \mp\frac{i\Sigma_L}{\sqrt{\Sigma_{LR}^2 - \Sigma_L^2 - \Sigma_R^2}}, \qquad (D.124)$$

$$G_R = \mp\frac{i\Sigma_R}{\sqrt{\Sigma_{LR}^2 - \Sigma_L^2 - \Sigma_R^2}}. \qquad (D.125)$$

So the wormhole saddle still presents [9]

$$G_L = G_R = \Sigma_L = \Sigma_R = 0, \quad G_{LR} = \pm i, \qquad (D.126)$$

$$e^{S_{eff}}\Big|_{WH} = e^{i^q TN\frac{t}{q}}. \qquad (D.127)$$

The unlinked half-wormhole saddle is:

$$G_{LR} = \Sigma_{LR} = 0, \quad G_L = \sin\alpha, \quad G_R = \cos\alpha, \quad (D.128)$$

$$e^{S_{eff}}\Big|_{unlink} = e^{TN\frac{u}{q}(\cos^q\alpha + \sin^q\alpha)}$$

$$\leq e^{S_{eff}}\Big|_{unlink,\alpha=0,\pi/2} = e^{TN\frac{u}{q}} \qquad (D.129)$$

where the relation

$$G_L^2 + G_R^2 - G_{LR}^2 = 1, \qquad (D.130)$$

is fulfilled and α satisfies

$$\cos\alpha = \pm\frac{\cos^{q-1}\alpha}{\sqrt{\cos^{2q-2}\alpha + \sin^{2q-2}\alpha}}. \qquad (D.131)$$

In the late time ($T \to \infty$), there is indeed a wormhole saddle so it possible to include a linked half-wormhole saddle for z. We also assume that the half-wormhole saddle is time independent since the wormhole saddle is time independent. Then the analysis is completely same as the one for the 0-dimensional model. So the half-wormhole saddle will be given by

$$\Theta = \left[\prod_i \theta_i\right]\int d^N\psi \exp\left(Ti^{q/2}\sum_A J_A\psi_A\right), \quad (D.132)$$

$$\langle\Theta^2\rangle \approx \langle\Theta z\rangle \approx \langle z_L z_R\rangle|_{Wormhole\ saddle}. \qquad (D.133)$$

References

1. J.M. Maldacena, The Large N limit of superconformal field theories and supergravity. Adv. Theor. Math. Phys. **2**, 231–252 (1998). https://doi.org/10.1023/A:1026654312961. arXiv:hep-th/9711200

2. E. Witten, Anti-de Sitter space and holography. Adv. Theor. Math. Phys. **2**, 253–291 (1998). https://doi.org/10.4310/ATMP.1998.v2.n2.a2. arXiv:hep-th/9802150

3. S.S. Gubser, I.R. Klebanov, A.M. Polyakov, Gauge theory correlators from noncritical string theory. Phys. Lett. B **428**, 105–114 (1998). https://doi.org/10.1016/S0370-2693(98)00377-3. arXiv:hep-th/9802109

4. G. Penington, Entanglement wedge reconstruction and the information paradox. JHEP **09**, 002 (2020). https://doi.org/10.1007/JHEP09(2020)002. arXiv:1905.08255 [hep-th]

5. A. Almheiri, N. Engelhardt, D. Marolf, H. Maxfield, The entropy of bulk quantum fields and the entanglement wedge of an evaporating black hole. JHEP **12**, 063 (2019). https://doi.org/10.1007/JHEP12(2019)063. arXiv:1905.08762 [hep-th]

6. A. Almheiri, R. Mahajan, J. Maldacena, Y. Zhao, The page curve of Hawking radiation from semiclassical geometry. JHEP **03**, 149 (2020). https://doi.org/10.1007/JHEP03(2020)149. arXiv:1908.10996 [hep-th]

7. G. Penington, S.H. Shenker, D. Stanford, Z. Yang, Replica wormholes and the black hole interior. arXiv:1911.11977 [hep-th]

8. P. Saad, S.H. Shenker, D. Stanford, JT gravity as a matrix integral. arXiv:1903.11115 [hep-th]

9. P. Saad, S.H. Shenker, D. Stanford, A semiclassical ramp in SYK and in gravity. arXiv:1806.06840 [hep-th]

10. P. Saad, Late time correlation functions, baby universes, and ETH in JT Gravity. arXiv:1910.10311 [hep-th]

11. C. Yan, Crosscap contribution to late-time two-point correlators. arXiv:2203.14436 [hep-th]

12. R. Bousso, X. Dong, N. Engelhardt, T. Faulkner, T. Hartman, S.H. Shenker, D. Stanford, Snowmass white paper: quantum aspects of black holes and the emergence of spacetime. arXiv:2201.03096 [hep-th]

13. J.M. Maldacena, L. Maoz, Wormholes in AdS. JHEP **02**, 053 (2004). https://doi.org/10.1088/1126-6708/2004/02/053. arXiv:hep-th/0401024

14. S.R. Coleman, Black holes as red herrings: topological fluctuations and the loss of quantum coherence. Nucl. Phys. B **307**, 867–882 (1988). https://doi.org/10.1016/0550-3213(88)90110-1

15. S.B. Giddings, A. Strominger, Baby universes, third quantization and the cosmological constant. Nucl. Phys. B **321**, 481–508 (1989). https://doi.org/10.1016/0550-3213(89)90353-2

16. S.B. Giddings, A. Strominger, Loss of incoherence and determination of coupling constants in quantum gravity. Nucl. Phys. B **307**, 854–866 (1988). https://doi.org/10.1016/0550-3213(88)90109-5

17. J. Polchinski, A. Strominger, A possible resolution of the black hole information puzzle. Phys. Rev. D **50**, 7403–7409 (1994). https://doi.org/10.1103/PhysRevD.50.7403. arXiv:hep-th/9407008

18. D. Stanford, E. Witten, JT gravity and the ensembles of random matrix theory. Adv. Theor. Math. Phys. **24**(6), 1475–1680 (2020). https://doi.org/10.4310/ATMP.2020.v24.n6.a4. arXiv:1907.03363 [hep-th]

19. L.V. Iliesiu, On 2D gauge theories in Jackiw–Teitelboim gravity. arXiv:1909.05253 [hep-th]

20. D. Kapec, R. Mahajan, D. Stanford, Matrix ensembles with global symmetries and 't Hooft anomalies from 2d gauge theory. JHEP **04**, 186 (2020). https://doi.org/10.1007/JHEP04(2020)186. arXiv:1912.12285 [hep-th]

21. H. Maxfield, G.J. Turiaci, The path integral of 3D gravity near extremality; or, JT gravity with defects as a matrix integral.

JHEP **01**, 118 (2021). https://doi.org/10.1007/JHEP01(2021)118. arXiv:2006.11317 [hep-th]

22. E. Witten, Matrix models and deformations of JT gravity. Proc. R. Soc. Lond. A **476**(2244), 20200582 (2020). https://doi.org/10.1098/rspa.2020.0582. arXiv:2006.13414 [hep-th]

23. I. Aref'eva, I. Volovich, Gas of baby universes in JT gravity and matrix models. Symmetry **12**(6), 975 (2020). https://doi.org/10.3390/sym12060975. arXiv:1905.08207 [hep-th]

24. P. Betzios, O. Papadoulaki, Liouville theory and Matrix models: a Wheeler DeWitt perspective. JHEP **09**, 125 (2020). https://doi.org/10.1007/JHEP09(2020)125. arXiv:2004.00002 [hep-th]

25. D. Anninos, B. Mühlmann, Notes on matrix models (matrix musings). J. Stat. Mech. **2008**, 083109 (2020). https://doi.org/10.1088/1742-5468/aba499. arXiv:2004.01171 [hep-th]

26. M. Berkooz, V. Narovlansky, H. Raj, Complex Sachdev-Ye-Kitaev model in the double scaling limit. JHEP **02**, 113 (2021). https://doi.org/10.1007/JHEP02(2021)113. arXiv:2006.13983 [hep-th]

27. T.G. Mertens, G.J. Turiaci, Liouville quantum gravity-holography, JT and matrices. JHEP **01**, 073 (2021). https://doi.org/10.1007/JHEP01(2021)073. arXiv:2006.07072 [hep-th]

28. G.J. Turiaci, M. Usatyuk, W.W. Weng, Dilaton-gravity, deformations of the minimal string, and matrix models. https://doi.org/10.1088/1361-6382/ac25df. arXiv:2011.06038 [hep-th]

29. D. Anninos, B. Mühlmann, Matrix integrals & finite holography. JHEP **06**, 120 (2021). https://doi.org/10.1007/JHEP06(2021)120. arXiv:2012.05224 [hep-th]

30. P. Gao, D.L. Jafferis, D.K. Kolchmeyer, An effective matrix model for dynamical end of the world branes in Jackiw–Teitelboim gravity. arXiv:2104.01184 [hep-th]

31. V. Godet, C. Marteau, From black holes to baby universes in CGHS gravity. JHEP **07**, 138 (2021). https://doi.org/10.1007/JHEP07(2021)138. arXiv:2103.13422 [hep-th]

32. C.V. Johnson, F. Rosso, A. Svesko, Jackiw–Teitelboim supergravity as a double-cut matrix model. Phys. Rev. D **104**(8), 086019 (2021). https://doi.org/10.1103/PhysRevD.104.086019. arXiv:2102.02227 [hep-th]

33. A. Blommaert, M. Usatyuk, Microstructure in matrix elements. arXiv:2108.02210 [hep-th]

34. K. Okuyama, K. Sakai, JT gravity, KdV equations and macroscopic loop operators. JHEP **01**, 156 (2020). https://doi.org/10.1007/JHEP01(2020)156. arXiv:1911.01659 [hep-th]

35. S. Forste, H. Jockers, J. Kames-King, A. Kanargias, Deformations of JT gravity via topological gravity and applications. arXiv:2107.02773 [hep-th]

36. A. Maloney, E. Witten, Averaging over Narain moduli space. JHEP **10**, 187 (2020). https://doi.org/10.1007/JHEP10(2020)187. arXiv:2006.04855 [hep-th]

37. N. Afkhami-Jeddi, H. Cohn, T. Hartman, A. Tajdini, Free partition functions and an averaged holographic duality. JHEP **01**, 130 (2021). https://doi.org/10.1007/JHEP01(2021)130. arXiv:2006.04839 [hep-th]

38. J. Cotler, K. Jensen, AdS$_3$ gravity and random CFT. JHEP **04**, 033 (2021). https://doi.org/10.1007/JHEP04(2021)033. arXiv:2006.08648 [hep-th]

39. A. Pérez, R. Troncoso, Gravitational dual of averaged free CFT's over the Narain lattice. JHEP **11**, 015 (2020). https://doi.org/10.1007/JHEP11(2020)015. arXiv:2006.08216 [hep-th]

40. N. Benjamin, C.A. Keller, H. Ooguri, I.G. Zadeh, Narain to Narnia. Commun. Math. Phys. **390**(1), 425–470 (2022). https://doi.org/10.1007/s00220-021-04211-x. arXiv:2103.15826 [hep-th]

41. J. Cotler, K. Jensen, AdS$_3$ wormholes from a modular bootstrap. JHEP **11**, 058 (2020). https://doi.org/10.1007/JHEP11(2020)058. arXiv:2007.15653 [hep-th]

42. M. Ashwinkumar, M. Dodelson, A. Kidambi, J.M. Leedom, M. Yamazaki, Chern–Simons invariants from ensemble averages.

43. N. Afkhami-Jeddi, A. Ashmore, C. Cordova, Calabi-Yau CFTs and random matrices. arXiv:2107.11461 [hep-th]

44. S. Collier, A. Maloney, Wormholes and spectral statistics in the Narain ensemble. arXiv:2106.12760 [hep-th]

45. N. Benjamin, S. Collier, A.L. Fitzpatrick, A. Maloney, E. Perlmutter, Harmonic analysis of 2d CFT partition functions. https://doi.org/10.1007/JHEP09(2021)174. arXiv:2107.10744 [hep-th]

46. J. Dong, T. Hartman, Y. Jiang, Averaging over moduli in deformed WZW models. https://doi.org/10.1007/JHEP09(2021)185. arXiv:2105.12594 [hep-th]

47. A. Dymarsky, A. Shapere, Comments on the holographic description of Narain theories. JHEP **10**, 197 (2021). https://doi.org/10.1007/JHEP10(2021)197. arXiv:2012.15830 [hep-th]

48. V. Meruliya, S. Mukhi, P. Singh, Poincaré series, 3d gravity and averages of rational CFT. JHEP **04**, 267 (2021). https://doi.org/10.1007/JHEP04(2021)267. arXiv:2102.03136 [hep-th]

49. R. Bousso, E. Wildenhain, Gravity/ensemble duality. Phys. Rev. D **102**(6), 066005 (2020). https://doi.org/10.1103/PhysRevD.102.066005. arXiv:2006.16289 [hep-th]

50. O. Janssen, M. Mirbabayi, P. Zograf, Gravity as an ensemble and the moment problem. JHEP **06**, 184 (2021). https://doi.org/10.1007/JHEP06(2021)184. arXiv:2103.12078 [hep-th]

51. J. Cotler, K. Jensen, Wormholes and black hole microstates in AdS/CFT. JHEP **09**, 001 (2021). https://doi.org/10.1007/JHEP09(2021)001. arXiv:2104.00601 [hep-th]

52. D. Marolf, H. Maxfield, Transcending the ensemble: baby universes, spacetime wormholes, and the order and disorder of black hole information. JHEP **08**, 044 (2020). https://doi.org/10.1007/JHEP08(2020)044. arXiv:2002.08950 [hep-th]

53. V. Balasubramanian, A. Kar, S.F. Ross, T. Ugajin, Spin structures and baby universes. JHEP **09**, 192 (2020). https://doi.org/10.1007/JHEP09(2020)192. arXiv:2007.04333 [hep-th]

54. J.G. Gardiner, S. Megas, 2d TQFTs and baby universes. JHEP **10**, 052 (2021). https://doi.org/10.1007/JHEP10(2021)052. arXiv:2011.06137 [hep-th]

55. A. Belin, J. de Boer, Random statistics of OPE coefficients and Euclidean wormholes. Class. Quantum Gravity **38**(16), 164001 (2021). https://doi.org/10.1088/1361-6382/ac1082. arXiv:2006.05499 [hep-th]

56. A. Belin, J. De Boer, P. Nayak, J. Sonner, Charged Eigenstate thermalization, Euclidean wormholes and global symmetries in quantum gravity. arXiv:2012.07875 [hep-th]

57. A. Altland, D. Bagrets, P. Nayak, J. Sonner, M. Vielma, From operator statistics to wormholes. Phys. Rev. Res. **3**(3), 033259 (2021). https://doi.org/10.1103/PhysRevResearch.3.033259. arXiv:2105.12129 [hep-th]

58. A. Belin, J. de Boer, P. Nayak, J. Sonner, Generalized Spectral Form Factors and the Statistics of Heavy Operators. arXiv:2111.06373 [hep-th]

59. C. Peng, J. Tian, J. Yu, Baby universes, ensemble averages and factorizations with matters. arXiv:2111.14856 [hep-th]

60. A. Banerjee, G.W. Moore, Comments on summing over bordisms in TQFT. arXiv:2201.00903 [hep-th]

61. C.V. Johnson, The microstate physics of JT gravity and supergravity. arXiv:2201.11942 [hep-th]

62. S. Collier, E. Perlmutter, Harnessing S-duality in $\mathcal{N} = 4$ SYM and supergravity as $SL(2, \mathbb{Z})$-averaged strings. arXiv:2201.05093 [hep-th]

63. J. Chandra, S. Collier, T. Hartman, A. Maloney, Semiclassical 3D gravity as an average of large-c CFTs. arXiv:2203.06511 [hep-th]

64. J.M. Schlenker, E. Witten, No ensemble averaging below the black hole threshold. arXiv:2202.01372 [hep-th]

65. R. Jackiw, Lower dimensional gravity. Nucl. Phys. B **252**, 343–356 (1985). https://doi.org/10.1016/0550-3213(85)90448-1

66. C. Teitelboim, Gravitation and Hamiltonian structure in two space-time dimensions. Phys. Lett. B **126**, 41–45 (1983). https://doi.org/10.1016/0370-2693(83)90012-6

67. S. Sachdev, J. Ye, Gapless spin fluid ground state in a random, quantum Heisenberg magnet. Phys. Rev. Lett. **70**, 3339 (1993). https://doi.org/10.1103/PhysRevLett.70.3339. arXiv:cond-mat/9212030

68. A. Kitaev, A simple model of quantum holography. Talks at KITP http://online.kitp.ucsb.edu/online/entangled15/kitaev/ and http://online.kitp.ucsb.edu/online/entangled15/kitaev2

69. A. Kitaev, "Hidden correlations in the Hawking radiation and thermal noise." Talk at KITP http://online.kitp.ucsb.edu/online/joint98/kitaev/

70. D. Stanford, More quantum noise from wormholes. arXiv:2008.08570 [hep-th]

71. A. Almheiri, H.W. Lin, The entanglement wedge of unknown couplings. arXiv:2111.06298 [hep-th]

72. P. Saad, S. Shenker, S. Yao, Comments on wormholes and factorization. arXiv:2107.13130 [hep-th]

73. P. Saad, S.H. Shenker, D. Stanford, S. Yao, Wormholes without averaging. arXiv:2103.16754 [hep-th]

74. B. Mukhametzhanov, Half-wormholes in SYK with one time point. arXiv:2105.08207 [hep-th]

75. A.M. García-García, V. Godet, Half-wormholes in nearly AdS$_2$ holography. arXiv:2107.07720 [hep-th]

76. S. Choudhury, K. Shirish, Wormhole calculus without averaging from $O(N)^{q-1}$ tensor model. arXiv:2106.14886 [hep-th]

77. B. Mukhametzhanov, Factorization and complex couplings in SYK and in Matrix Models. arXiv:2110.06221 [hep-th]

78. K. Okuyama, K. Sakai, FZZT branes in JT gravity and topological gravity. JHEP **09**, 191 (2021). https://doi.org/10.1007/JHEP09(2021)191. arXiv:2108.03876 [hep-th]

79. K. Goto, Y. Kusuki, K. Tamaoka, T. Ugajin, Product of random states and spatial (half-)wormholes. JHEP **10**, 205 (2021). https://doi.org/10.1007/JHEP10(2021)205. arXiv:2108.08308 [hep-th]

80. A. Blommaert, L.V. Iliesiu, J. Kruthoff, Gravity factorized. arXiv:2111.07863 [hep-th]

81. K. Goto, K. Suzuki, T. Ugajin, Factorizing wormholes in a partially disorder-averaged SYK Model. arXiv:2111.11705 [hep-th]

82. C. Peng, Ensemble averages, Poisson processes, and microstates. Phys. Rev. D **103**(6), L061901 (2021). https://doi.org/10.1103/PhysRevD.103.L061901. arXiv:2010.11192 [hep-th]

83. E. Witten, Analytic continuation Of Chern–Simons theory. AMS/IP Stud. Adv. Math. **50**, 347–446 (2011). arXiv:1001.2933 [hep-th]

84. C. Peng, J. Tian, Y. Yang, Half-wormholes and ensemble averages. arXiv:2205.01288 [hep-th]

85. N.N. Bogolyubov, On the theory of superfluidity. J. Phys. (USSR) **11**, 23–32 (1947)

86. J.G. Valatin, Comments on the theory of superconductivity. Nuovo Cim. **7**, 843–857 (1958). https://doi.org/10.1007/BF02745589

87. J. Tian, Y. Yang, More on half-wormholes and ensemble average. arXiv:2211.09398 [hep-th]